ABSTRACT

Wang, Zhi. Spectral Analysis of Protein Sequences. (Under the direction of Dr. William R. Atchley and Dr. Charles E. Smith.)

The purpose of this research is to elucidate how to apply spectral analysis methods to understand the structure, function and evolution of protein sequences.

In the first part of this research, spectral analyses have been applied to the basic-helix-loop-helix (bHLH) family of transcription factors. It is shown that the periodicity of the bHLH variability pattern (entropy profile) conforms to the classical α-helix periodicity of 3.6 amino acids per turn. Further, the underlying physiochemical attributes profiles (factor score profiles) are examined and their periodicities also have significant implications of the α-helix secondary structure. It is suggested that the entropy profile can be well explained by the five factor score variance components that reflect the polarity/hydrophobicity, secondary structure information, molecular volume, codon composition and electrostatic charge attributes of amino acids.

In the second part of this research, complex demodulation (CDM) method is introduced in an attempt to quantify the amplitude of periodic components in protein sequences. Proteins are often considered to be "multiple domain entities" because they are composed of a number of functionally and structurally distinct domains with potentially independent origins. The analyses of bZIP and bHLH-PAS protein domains found that complex demodulation procedures can provide important insight about functional and structural attributes. It is found that the local amplitude

minimums or maximums are associated with the boundary between two structural or functional components.

In the third part of this research, the periodicity evaluation of a leucine zipper protein domain with a well-known structure is used to rank 494 published indices summarized in a database (http://www.genome.jp/dbget/aaindex.html). This application allows us to select those amino acid indices that are strongly associated with the protein structure and hereby to promote the protein structure prediction. This procedure can be used to reduce some redundancy of the amino acid indices.

Spectral Analysis of Protein Sequences

by

Zhi Wang

A dissertation submitted to the Graduate Faculty of
North Carolina State University
in partial fulfillment of the
requirements for the Degree of
Doctor of Philosophy

Biomathematics and Bioinformatics

Raleigh
2005

APPROVED BY:
Chair of Advisory Committee

Chair of Advisory Committee

Co-Chair of Advisory Committee

Biography

I was born in Wuhan, Hubei, China on Mar 18, 1977. I attended the No. 1 Middle School of Chinese Central Normal University, where I was intrigued by the complexity of life. As a teenager, I became enamored with science and math and participated contests of biological science. I attended Wuhan University in the fall of 1994 and majored in Biology. In 1998, I was awarded the Bachelor Degree. In 2000, I was awarded a Master Degree in Genetics. During this period, I was proud of publishing one scientific paper on modeling of branching structures of plants and accomplishing the computer simulation of genetic recombination project. After encouragement and support from Youhao Guo and Qixing Yu, I decided to apply and later attend North Carolina State University for my graduate studies on Biomathematics and Bioinformatics. Fortunately, I begin working in William Atchley's lab on computational biology and I am able to do a lot exploration works on computational methods under the guidance of Dr. Atchley and Dr. Smith. The following thesis will explain what I have been doing during these last few years in Atchley's lab.

Acknowledgements

There are many people who have been very helpful throughout my graduate career. First and for most I would like to thank my advisor Dr. William R. Atchley and Dr. Charles E. Smith, for academic mentoring and for allowing me to do exploratory research on computational biology. I would like to thank all my committee members past and present Dr. Bruce S. Weir and Dr. Jeff L. Thorne.

For emotional support I would like to thank my fellow graduate students especially Jieping Zhao, Andrew Fernandes, Kevin Scott, Andrew Dellinger and Jhondra Funk-Keenan. I wish to thank my parents Dashun Wang and Yingqing Liu for their love and financial support. Lastly, I am indebted to my wife Jing Zhang for her love and support.

Table of Contents

Page

List of Tables

Page

List of Figures

Page

Introduction

Spectral Analysis

The broad application of genome sequencing methodology has generated a huge amount of protein sequence data. Parallel development of sophisticated computational and statistical methodology for analyzing sequence data has equipped us with many tools to investigate and explore protein evolution as well as the relationship between protein sequence and structure. Of particular importance has been the application of methodology permitting simultaneous consideration of many amino acid sites to elucidate “patterns” of variability over large portions of particular proteins. Often such multivariate analyses have focused on the multidimensional patterns of covariation among amino acid sites.

An integral part of analyzing the multidimensional nature of sequences is the description of periodicity in the attributes among sequence elements. Periodicity of sequence elements can reveal important structural and functional characteristics of the molecule. A typical method for studying periodicity is spectral analysis, which characterizes the frequency content of a measured signal. Spectral analysis has been widely used to analyze time series data, and indeed can be used to analyze protein sequences data if the amino acid is represented by numeric values. There are many kinds of spectral analysis methods, including Fast Fourier Transformation (FFT) method, Yule-Walker method, Burg method, Least Squares method and

Maximum likelihood method as well (Marple, 1987; Percival and Walden, 1993).

The FFT method has a number of advantages over other methods. (i) The only assumption FFT makes is that the data are wide-sense stationary. However, the non-classical methods require additional assumptions. Only when the non-classical model is an accurate representation of the data, these spectral estimates can outperform the classical spectral estimators (e.g., the periodogram) (Marple, 1987). (ii) Statistical property of the periodogram method has been well addressed over other methods (Percival and Walden; 1993). The FFT is more easily interpreted in terms of partitioning of variance (Warner, 1998). (iii) The FFT algorithm is the most computationally efficient spectral estimation method available (Marple, 1987).

The FFT method has been used to detect the residue repeat of a protein sequence (Mclachlan,1977) and a web server designed for locating periodical pattern of a sequence exists (Pasquier *et al.*, 1998). In the latter case, a sequence of *N* residues is represented as a linear array of *N* items, with each item given a weight. The sequence of weights is used to create a "pulse", which can be analyzed by Fourier analysis. For example, selecting a weight of 1 for "*D*" and 2 for "*L*", the sequence '*AAILVADMLIA*' is transformed into the array {0 0 0 2 0 0 1 0 2 0 0}. In Fourier theory such numeric array pattern can be decomposed into a number of sine and/or cosine waves, consisting of integer multiples of the basic frequency. The period is the same as the inverse of the frequency.

Other methods have been proposed because of the low-resolution limitation of the FFT method. These include the Yule-Walker method, the Burg method, the Least Squares method and the Maximum likelihood method. All of these methods are based on parametric spectral estimation and hereby they can compensate for the low-resolution of FFT method. They can maintain or improve high resolution without sacrificing stability (Marple, 1987; Naidu, 1996).

Few applications of spectral analysis methods to the protein sequences have been reported. Therefore, in Chapter 1, both the FFT method and the Burg method are applied to conduct spectral analyses to the variability profiles of the basic-helix-loop-helix (bHLH) protein domains. Rigorous statistical tests have been included in this research. The Burg method was explored over other methods because: (i) The Burg method is computationally more efficient than the Maximum Likelihood method (Kay 1988, Percival and Walden, 1993). (ii) The Burg method produces stable and more reasonable estimates for short data series, which is useful in studying short protein sequences (Matlab Help 2004, Percival and Walden, 1993).

Warner (1998) recommends some preliminary data analysis on the sequence data before the spectral analysis. First, it is recommended determining whether there is a linear trend (change in level over residues). If a trend is present, it needs to be removed before assessing periodic component. Second, it is recommended that one ascertain if the data series is stationary. If the stationary assumption is violated, an overall FFT or spectral analysis on the entire data series can be somewhat misleading. In the latter instance, the complex demodulation method described in the Chapter 2 is suggested. Third, it is recommended that one determine if the data series represents white noise, i.e., observations uncorrelated with each other. In the context of spectral analysis, white noise means no individual periodic component explains a larger share of the variance than the other periodic component. The spectrum shows a flat line under the null hypothesis. Finally, one conducts the spectral analysis with FFT method or others to protein sequences and analyzes the results.

Variability Profiles in Entropy and Factor Scores

To accurately and robustly define the variability of alphabetic data, we apply tools from information theory. Specifically, we use entropy profiles to measure the residue diversity of each amino acid in multiple alignments. Entropy profile procedures are widely accepted in many fields of science and are frequently employed in physics, chemistry, biology, mathematics, statistics, etc. (Atchley, 1997, 1999, 2000, 2005). Once one has accurately described differential variability in a set of aligned sequences with entropy profile, the next step is to resolve the origin and underlying causality of the observed sequences variability. We need to understand the underlying physiochemical causes of sequence variability, not simply describe them as a “molecular natural history” phenomenon.

However, there are serious statistical problems associated with analyzing the amino acid variability in biological sequence data, the so-called “sequence metric problem” (Atchley, 2005). Protein sequences are composed of long strings of alphabetic letters rather than arrays of numerical values. Lack of a natural underlying metric for comparing such alphabetic data significantly inhibits sophisticated statistical analyses of sequences, modeling structural and functional aspects of proteins, and related problems. For example, the amino acid leucine (L) is more similar in its physiochemical properties to valine (V) than leucine is to alanine (A). Currently, no reliable quantitative measure exists to summarize the extent of the physiochemical divergence among amino acids. These differences must be quantified before periodicity analysis of physiochemical variability can be understood for protein sequences.

Previous authors circumvented sequence metric problems in different ways. Some generated ad hoc quantitative indices to summarize amino acid variability (Grantham, 1974; Sneath, 1966). However, ad hoc indices generally summarize only part of the total variability in amino acid attributes. If a numerical index approach is to be effective, indices must (i) represent the proximate causes of amino acid variability; (ii) reflect interpretable partitions of total amino acid variation; and (iii) resolve intercorrelations among relevant amino attributes (Atchley *et al*, 2005).

An on-line database (AAIndex) exists that summarizes many attributes of amino acids (www.genome.ad.jp/dbget/aaindex.html). A total of 494 indices are found at this website that include general attributes, such as molecular volume or size, hydrophobicity, and charge, as well as more specific measures, such as the amount of nonbonded energy per atom or side chain orientation angle.

However, there is much redundancy in these data making selection of appropriate indices for analyses much more difficult Atchley et al. (2005) used the multivariate statistical procedure of factor analysis to produce a subset of numerical descriptors that would summarize the entire constellation of amino acid physiochemical properties. Factor analysis is a powerful exploratory statistical procedure, that can simplify high-dimensional data by generating a smaller number of ‘‘factors’’ that describe the structure of highly correlated variables. The resultant factors are linear functions of the original data, fewer in number than the original, and reflect clusters of covarying traits that describe the underlying or ‘‘latent structure’’ of the variables. High-dimensional attribute data are summarized by five multidimensional patterns of attribute covariation that reflect polarity, secondary structure, molecular volume, codon diversity, and electrostatic charge.

Thus, the entropy profiles and factor scores permit me to conduct spectral analysis on the periodicity of proteins to investigate their structure, function and evolution in this dissertation.

Complex Demodulation

Suppose that a set of data contains a perturbed periodic component $X_t = A_t \cos(\lambda t + \phi_t) + z_t$ where A_t is a slowly changing amplitude instead of a constant, and ϕ_t is a slowly changing phase. Complex demodulation is to extract approximations to the series A_t and ϕ_t. Description of the amplitude and the phase of a particular frequency by rigorous mathematical tools can be very informative to solve the puzzle of the complicated structure and function of protein sequences. However, spectral analyses, such as those based on the FFT method, cannot be used to assess sudden, time-dependent (i.e. amino acid site-dependent for protein sequences) changes in the amplitude of a particular frequency.

The complex demodulation method (CDM) has been developed to provide a continuous assessment of the amplitude of numeric protein sequences and thereby identify changing events (Bloomfield, 1976). While CDM has been widely applied in many other scientific field (Hayano, *et al*., 1993; Lipsitz, *et al*., 1998; Babkoff, *et al*., 1991; Rutherford and D'Hondt, 2000), it has apparently never been applied in computational biology and bioinformatics. I explored the application of CDM on the entropy and factor profiles of basic-ZIP (bZIP) and basic-Helix-Loop-Helix-PAS (bHLH-PAS) protein domains. These results are summarized in Chapter 2.

Currently there are several on-line bioinformatics tools of analyzing the hydrophobicity profiles of protein sequences. For example, the tool at http://arbl.cvmbs.colostate.edu/molkit/hydropathy can make plots that characterize the hydrophobic character of protein sequences, which may be useful in predicting membrane-spanning domains, potential antigenic sites and regions that are likely exposed on the protein's surface. Generally, windowing techniques have been used in analyses of the hydrophobicity profiles where window size refers to the number of amino acids examined to determine hydrophobic characteristics. Windowing techniques can smooth the hydrophobicity profiles and reduce fluctuation in the original signal. Unfortunately, such procedures result in the loss of some biological information, especially the information contained in the high-frequency components. In other words, the removal of short-range oscillations results in the loss of some biological information.

The CDM method is a mathematical tool that can be used to analyze the amplitude and phase of the high-frequency components without the loss of information because it does not use windowing techniques. Therefore, it can be regarded as a complementary procedure to other computational tools of analyzing sequence profiles. Indeed, it can also analyze low-frequency components. The analyses of the changing amplitude of the 3.6-aa periodic component of bZIP and bHLH-PAS protein domains in Chapter 2 prove that CDM is a sound procedure to reveal the biological information contained in high-frequency components.

Evaluation of Amino Acid Indices

Interaction with water of the amino acid side chains is a major determinant of protein structure. The hydrophobic scales are semiempirical quantities based on both computation and experimental measurements that describe the interaction between amino acid and water. The hydrophobic scales are helpful in analyzing the protein biochemical structures because they are associated with the free energy of folding and formation of structure (Fasman,1989). However, there are numerous indices proposed to measure residue hydrophobicity and there is a lot of redundancy of these indices.

In Chapter 3, periodicity evaluation is proposed as a method to make comparison among those indices that are closely associated with the helix formation. If the periodicity of a certain amino acid index profile conforms to the observed periodicity of a well-known structure, then such amino acid index can be assumed as a good one.

Goal of Research

The application of spectral analysis methods on protein sequences is poorly investigated. Therefore, the goal of my dissertation work is to explore the potential application of these methods.

This research is to demonstrate how spectral analysis methods such as FFT, Burg method and complex demodulation can be used to analyze the biological signals contained in protein sequences. This research is to elucidate that the entropy profile can be decomposed into underlying physiochemical components. This research is to elucidate that the complex demodulation method is a promising method to quantify the amplitudes of periodic components of protein sequence signals. And the research suggests that the amplitudes are predictors of protein structure and function. Finally, this research presents an approach to rank the amino acid indices based on their periodicity parameters, which is valuable to determine the best amino acid index for computation.

Chapter 1

Spectral Analysis of Sequence Diversity in basic-Helix-Loop-Helix (bHLH) Protein Domains

by

Zhi Wang[1,*] and William R. Atchley[1,2]

[1]Graduate Program In Biomathematics And Bioinformatics and [2]Department Of Genetics and Center For Computational Biology, North Carolina State University, Raleigh, NC 27695-7614, USA

Key words: spectral analysis, entropy, factor, periodicity, helix

[*] To whom correspondence should be addressed

[*] CONTACT: zwang2@ ncsu.edu

ABSTRACT

Using the basic helix-loop-helix (bHLH) family of transcription factors as a paradigm, we explore whether periodicity patterns of amino acid diversity have implications of its helix secondary structure. Further we wish to ascertain whether statistical analyses will clarify the underlying causes of periodic amino acid variation. A Boltzmann-Shannon entropy profile was used to represent site-by-site amino acid diversity in the bHLH domain. Spectral analysis showed that the periodicity of the bHLH entropy profile and provided strong statistical evidence that the amino acid diversity pattern conforms to the classical α-helix three-dimensional structure periodicity of 3.6 amino acids per turn. Then, amino acid attribute indices derived from multiple factor analysis of almost 500 amino acid attributes were used to explore the underlying causal components of the bHLH variability patterns. These five multivariate attribute indices reflect patterns in i) polarity / hydrophobicity / accessibility, ii) propensity for various secondary structures, iii) molecular volume, iv) codon composition and v) electrostatic charge. The periodicity analyses of these indices also have significant implications of the underlying helix secondary structure. Further, multiple regression analyses of the entropy values and the underlying physiochemical attributes represented by factor score means/variances can decompose the variation in entropy values into their underlying structural components. These analyses have significant implications of the statistical estimations of important attributes of protein secondary structure.

Availability: http://www.atchleylab.org/spectral/bhlh.htm

Introduction

Much of contemporary research in biological, medical and agricultural sciences focuses on complex traits. Complex traits are generally characterized as being composed of various component parts that are interdependent, dynamic and multi-regulated. Some classic examples include mammalian body weight, craniofacial form, human diseases like diabetes, heart disease and cancer, human behaviors like schizophrenia and alcohol addiction, and other important traits. Protein molecules often fit this classification as well. Protein molecules: i) may contain multiple structural and functional domains, ii) protein domains are composed of many different amino acid sites with varying degrees of intercorrelation, iii) the various amino acids contribute differentially to structure and function, iv) the separate domains may have distinct evolutionary origins, v) they are integrated through processes like domain shuffling, and vi) different domains (and their constituent amino acids) may be subjected to separate selection regimes based on their functioning. To adequately understand protein evolution and structure requires a deeper knowledge of these component parts of proteins, their characteristics, dynamics, integration and divergence.

In a series of papers, we have employed a computational biology approach to exploring a number of structural and evolutionary aspects of the basic helix-loop-helix (bHLH) family of proteins. The bHLH proteins are a collection of important transcriptional regulators that are involved with the control of a wide variety of developmental processes in eukaryote organisms (Murre *et al*., 1989, 1994; Sun and Baltimore, 1991; Atchley and Fitch, 1997; Ledent and Vervoort, 2001).

Our previous analyses have focused on a number of important questions including estimating amino acid diversity, describing phylogenetic relationships (Atchley and Fitch, 1997), elucidating networks of covarying amino acid sites (Atchley *et al*., 2001; Buck and Atchley, 2005), describing the relationships between sequence covariability and protein structure (Atchley *et al*., 2001), exploring the underlying causes of sequence covariation (Wollenberg and Atchley, 2000; Atchley *et al*., 2001), describing sequence signatures (Atchley *et al*., 2000; Atchley and Fernandes, 2005), exploring domain shuffling (Morgenstern and Atchley, 19xx) and other fundamental questions about this important group of proteins. In all of these analyses, we have sought to provide results and methodology that can be incorporated in results of other types of structural and functional analyses.

Herein, we use a battery of computational methods to explore the nature of amino acid diversity in the bHLH proteins to better understand the underlying causes of sequence variability and covariability. Specifically, we wish to ascertain whether the patterns of amino acid diversity in the bHLH domain over large numbers of sequences (as shown by Atchley *et al*., 2000) correspond to the structural geometry of single proteins, as described by crystal structure studies (e.g., Ferre-D'Amare *et al*., 1993; 1998 Shimizu *et al*., 1997). Previously, we have used a mutual information approach to describe differential variability and covariability among amino acid sites in large aligned sequence databases (Atchley *et al*., 1999, 2000; Wollenberg and Atchley, 2000). In the present paper, we evaluate the null hypothesis that the observed patterns of amino acid diversity in the bHLH domain exhibit a systemic *periodicity* that corresponds to known structural geometry.

A number of previous authors have suggested that analyses of periodicity among sequence elements can elucidate important characteristics in molecular structure, function and evolution (Eisenberg *et al.*, 1984; Pasquier *et al.*, 1998; Leonov and Arkin, 2005). For example, an α-helix adopts an amino acids spiral configuration of $99^\circ \pm 7^\circ$ around the helical axis, generating a range in periodocity of 3.40 - 3.91 aa per turn. The conventionally accepted average periodocity value is about 3.60 aa per turn (Kyte, 1995). Mutations that disrupt such structural geometry are expected to be subject to strong natural selection (Patthy, 1999). Hence, there should be significant changes in the patterns of amino acid diversity at different positions in the α-helix that are conserved over large numbers of evolutionarily related proteins. Indeed, our previous quantitative analyses of the bHLH domain suggest a strong relationship between levels of amino acid diversity and the amphipathic nature of the α-helices that comprise the bHLH domain (Atchley *et al*., 2000).

Herein, we use spectral analysis, information theory and multivariate statistical methods to examine the periodic nature in amino acid variability in the bHLH domain. Our goal is to: 1) describe the periodicity patterns in amino acid diversity within the highly conserved bHLH protein domain; 2) ascertain whether the diversity in amino acid composition conforms to estimates of secondary structure known from previous crystal structure analyses; and 3) decompose the variability in entropy patterns into their underlying structural components.

Methods

Definition and Structure of the bHLH Domain

The bHLH domain is a highly conserved domain comprised of approximately 60 amino acids (Atchley and Fitch, 1997). It is best modeled as two separate α-helices separated by the loop (Ferre-D'Amare *et al.*, 1993; Shimizu *et al.*, 1997). The domain is comprised of a basic DNA binding region (b) of about 14 amino acids that interacts with a consensus hexanucleotide E-box (CANNTG). The basic region is followed by two amphipathic α-helices (H) separated by a variable length loop (L). The helix regions are involved with protein-DNA contacts and protein-protein interaction, i.e., dimerization. The loop region is of variable length and may range from approximately 5 to 50 residues that are generally quite difficult to homologize among different bHLH subfamilies (Morgenstern and Atchley, 1999)

The bHLH proteins are conventionally classified into 5 major DNA-binding groups (A, B, C, D, and E) based on how the proteins bind to the consensus E-box and other attributes (Atchley and Fitch, 1997; Ledent and Vervoort, 2001). Herein, we analyze a total of 196 bHLH sequences chosen to reflect the diversity of the bHLH subfamilies and DNA binding groups. These data include 83, 72, 16, 9 and 16 sequences belonging to groups A, B, C, D and E, respectively. These sequences are part of a standard bHLH dataset used in a number of previous computational analyses (Atchley and Fitch, 1997; Atchley *et al*., 2000; Atchley *et al*., 2005).

Data preparation

The sequences were initially aligned using both local and global type alignment algorithms and the resultant preliminary alignments then corrected by eye when the results of the two alignment algorithms did not agree. Representatives of the aligned subfamilies can be found in Atchley and Fitch (1997). As is previous analyses, the break points between components follows the structural analyses of Ferre-D'Amare *et al*., (1993). where the basic region includes amino acids 1—13; helix 1 involves 14—28; the loop comprises 29—49 and helix 2 includes 50—64.

To facilitate subsequent analysis, the loop region between residues 32 and 46 was removed. The loop region is highly divergent in both length and composition among groups of bHLH proteins making accurate decisions about homology difficult for much of this region Atchley and Fitch, 1997; Morgenstern and Atchley, 1999). Unless an accurate alignment can be achieved, subsequent statistical analyses are of dubious value. Thus, much of the loop has been removed and only 49 columns of the multiple alignments remain further spectral and statistical analysis. Removal of the non-homologous portion before subsequent analyses is standard procedure for such analyses. Preliminary spectral density plots of the profile containing the whole loop region was compared with the one used in this paper. The results were not significantly affected by removing this highly variable portion of the loop region.

Additional analyses can be found at *http://www.atchleylab.org/spectral/bhlh.htm*

Entropy Profiles

We use the Boltzmann-Shannon entropy *E* to quantify sequence variability of amino acid residues at each aligned amino acid site as defined in Atchley *et al.* (1999, 2000). It is calculated as $E(p) = -\sum_{j=1}^{21} p_j \log_2(p_j)$, where p_j is the probability of a residue being a specific amino acid or a gap, and $0 \le E(p) \le 4.39$. An "entropy profile" is given in a histogram (Fig.1.2a) where the height of the individual bars reflects the entropy value (residue diversity) at a particular aligned amino acid site. Small E values indicate a high degree of sequence conservation.

Factor Score Profiles

Atchley *et al.* (2005) pointed out that statistical analyses of alphabetic sequence data are hindered by the lack of a rational underlying metric for alphabetic codes. To resolve this "metric" problem, these authors generated a small set of highly interpretable numerical values that summarize complex patterns of amino acid attribute covariation. This was accomplished through multivariate statistical analyzes of 495 separate amino acid attributes and. Using factor analysis (Johnson and Wichern 2002), these authors defined five major patterns of amino acid attribute covariation that summarize the most important aspects of amino acid covariability. These five patterns or multidimensional indices were interpreted as follows: Factor I = a complex index reflecting highly intercorrelated attributes for polarity, hydrophobicity, solvent accessibility, etc. Factor II = propensity to form various secondary structures, e.g., coil, turn or bend versus alpha helix frequency. Factor III = molecular size or volume, including bulkiness, residue volume, average volume of a buried residue, side chain volume, and molecular weight. Factor IV = relative amino acid composition in various proteins, number of codon coding for an amino acid, and amino acid composition. Factor V = electrostatic charge including isoelectric point and net charge. A set of *"factor scores"* arising from these analyses provide a multidimensional index positioning each amino acid in these major interpretable patterns of physiochemical variation.

Herein, we transform the original alphabetic amino acid codes to these five factor scores in the aligned sequence data. This procedure generates five sets of numerical values that accurately reflect a broad spectrum of amino acid attributes. The factor score transformed data is then used for many of our subsequent statistical analyses. For simplicity, we analyze the five factor score transformed data individually, i.e., one set of analyses for polarity/hydrophobicity, another for molecular size, etc, rather than do an analysis of all five factors simultaneously.

To better understand the underlying causes of diversity in amino acids, we include analyses of both the factor score means as well as the factor variances (Fig.1.2.b-k). The former replaces alphabetic data with the average amino acid attribute while the latter uses a multidimensional measure of attribute variability.

Spectral Analysis Based on Fourier Transformation

It is well known that amino acid sequences can exhibit a periodic pattern in the occurrence of certain types of amino acids. What is not clear is whether the diversity of site-specific amino acids similarly exhibits periodic patterns.

To explore this question, a time series model can be expressed in terms of sine and cosine components (Bloomfield, 1976) as

$$Y_t = \sum_{i=1}^{m} (A_i \cos(\omega_i t) + B_i \sin(\omega_i t)) + e_t \qquad (1)$$

where Y_t is the original variable with n observations. $m=n/2$ if n is even; $m=(n-1)/2$, if n is odd. ω_i specifies the Fourier frequencies, $2\pi i/n$, where i =1, 2, …, m. A_i and B_i are the amplitude of the sine and cosine components. e_t is the error term.

The sum of squares of the A_i and B_i can be plotted against frequency or against wavelength to form periodograms. The periodogram can be interpreted as the amount of variation in Y at each frequency. If there is a significant sinusoidal component at a given frequency, the amplitude A or B or both will be large and the periodogram will have a large ordinate at that given frequency. If there is no significant sinusoidal component, then the periodogram will not have any large ordinates at any frequencies. Hamming window is applied to produce the spectral density plots, which is a general smoothing procedure in spectral analysis (Kendall and Ord, 1990). The spectral density plots (Fig.1.3) of entropy, factor score means and variances are produced by the Fast Fourier Transformation (FFT) procedure in SAS software (PROC SPECTRA).

With Fourier Transformation, any waveform can be analyzed as a combination of sine waves of various amplitude, frequency and phase. For example, a signal which is a sum of sin(x) and 2cos(3x) can be analyzed by its spectral plot, in which there are two bars representing these two periodic components (Fig. 1.1).

Spectral Analysis Based on the Burg Method

The Burg method is a spectral analysis procedure based on the well-known autoregressive (AR) modeling technique for processing time-series data (Marple, 1987; Kay, 1988). An AR model provides a parametric description for the time-series data being analyzed. For a given discrete data sequence x_i for 1 ⩽ i ⩽ n, the sample at index i can be approximated by a linear combination of previous k observations of the data sequence by $X_i = \hat{X}_i + e_i = -\sum_{k=1}^{k} \hat{a}_k X_{i-k} + e_i$ where $i \geq k$. In the Burg method, the spectral density of the time series can be described in terms of AR model parameters and the corresponding modeling error variance by

$$\hat{P}_{AR}(f) = \frac{T\hat{\sigma}^2}{\left|1 + \sum_{i=1}^{p} \hat{a}_i \exp(-j2\pi fnT)\right|^2} \qquad (2)$$

$$j^2 = -1$$

where $\hat{\sigma}^2$ is the estimated modeling error variance, and *T* is the sampling interval.

The Burg method is used to calculate the spectral density of the entropy and factor score variance series as an alternative method to the FFT method. Readers are referred to Marple (1987) for more details on the algorithms of the Burg method. Similar to the Fourier transformation method, the spectral density plot can be produced by the Burg method. The spectral density plots for entropy, factor score means and variances profiles produced by Matlab software (version 6.5) are very similar to those listed in Fig.1.3 produced by FFT method.

When spectral density plots are graphed, “large” peaks are generally noted, necessitating determination of their statistical significance and accuracy. Several follow-up analyses were conducted to gain more information out of the spectral density plots.

Fisher’s test is a useful and conservative test for identification of “major” periodic components (Warner, 1998). The premise behind the Fisher’s test rejection of the null hypothesis if the periodogram contains a value significantly larger than the average value (Brockwell and Davis, 1991; Warner, 1998). The test statistic *g*, gives the proportion of the total variance that is accounted for by the largest periodogram component. The critical values of the proportion of variance for the Fisher’s test at α=0.05 level (N=49) are 0.240, 0.156 and 0.122 for the first, second and third largest periodogram ordinates, respectively. The critical value 0.240 means that if there are 49 data points in the numeric sequence, then the largest periodogram ordinate must account for more than 24% of the variance to by judged significant at the 0.05 level. Note that in the special case of a constant time series (constant numeric sequence in this paper), the *p*-value returned by Fisher's test is exactly 1 (i.e. the null hypothesis is not rejected). If the largest periodogram ordinate is statistically significant, then it is possible to go on and test the second and third largest periodogram ordinates for significance, and so on.

Given the major periodic components, harmonic analysis was used to fit the data with the cyclic components (Warner, 1998). As in regression analysis, harmonic analysis involves estimating the amplitude parameters *A* and *B* in the formula (1) given a fixed fundamental period parameter *ω*. *R*-square (R^2) measures the goodness of fit of the predictive model and estimates the percentage of total variance of the observations explained by the analysis. Therefore, with the period estimate from the spectral analysis as a prior, we are able to search for the best period estimate maximizing the *R*-square in a relative small range and its confidence interval (CI).

For the entropy profile, a bootstrap simulation procedure is used to produce 1000 random samples with replacement from the original bHLH multiple alignments. For each sample, the harmonic analysis is conducted to detect the best period estimate with the largest *R*-square statistics. Assuming the 1000 period estimates have a normal distribution, the 95% confidence interval of the mean can be obtained.

Analysis of variance (ANOVA) is conducted to partition the total variance in the entropy data into the variance in factor scores for Factors I-V. The null hypothesis in this analysis is that there is no difference between the total variation of the scores for Factor I-V and the error variance.

Further, multiple regression analysis is conducted (dependent variable: entropy independent variable: five factor score variance components) to estimate β_0, β_1,…, β_5 of the following regression model equation.

$$\text{Entropy} = \beta_0 + \beta_1(\text{Factor I Var}) + \beta_2(\text{Factor II Var}) + \beta_3(\text{Factor III Var}) + \beta_4(\text{Factor IV Var}) + \beta_5(\text{Factor V Var}) + \varepsilon \qquad (3)$$

where ε is a normal distributed random variable with μ_ε=0 and $\sigma_\varepsilon^2=\sigma^2$

RESULTS

Periodicity Analyses of Entropy Profiles

The spectral density plot produced by the Fast Fourier transformation for the entropy profile is shown in Fig.1.3a. The largest peak corresponds to a period of approximately 3.77 aa. The spectral density plot produced by the Burg method is very similar. Fisher's test indicates that the periodogram ordinate at 3.77 aa is significantly different from the average periodogram, which confirms that the periodic component with a period of 3.77aa is statistically significant. However, the second and third largest periodogram ordinates are not significant. Thus, there is one statistically significant major periodicity component in the entropy profile and it corresponds to a value well within the range of known α-helix values.

Limitations of the Fourier frequency reported by the FFT method permit the spectral analysis to give only an approximate periodicity estimate. Thus, harmonic analysis was conducted to detect the best period estimate in the range from 3.30 aa to 3.90 aa, with increments of 0.01. A predictive model was fitted and the associated *R*-square statistics (R^2) was calculated each iteration. The period maximizing the *R*-square statistics was recorded as the best period estimate. Results indicate that the entropy profile has a major periodic component of 3.6776 aa repeat and this component can explain 45.7% of total variance (R^2 = 0.457).

A 95% confidence interval of the period estimate calculated from 1000 bootstrap entropy profiles gives an interval of (3.6773 - 3.6778). This finding substantiates our result that there is a major periodic component in the entropy profile of bHLH protein domain. Thus, the entropy profile of bHLH protein domain has a periodicity estimate very similar to the conventionally accepted value (3.60 aa per turn) for the ideal α-helix.

Periodicity of Factor Score Means

The factor score means describe the average physiochemical attribute for each amino acid site for each factor (=multidimensional physiochemical attribute index). The spectral density plot of Factor I (polarity) means is given in Fig.1.3b. The peaks located between 3-4 aa suggest the existence of periodic components. The periodogram data suggests three possible periodic components of 3.27 aa, 3.77 aa and 2.58 aa. The Fisher's test statistic *g* for the 3.27-aa periodic component is 0.196, which does not exceed the critical value 0.240. However, if it is assumed that the 3.27-aa component is significant and we continue to test the 3.77-aa component, it is found that the Fisher's test statistics *g* of the 3.77-aa periodic component is 0.176, which exceeds the critical value 0.156. These results suggest that there are possible significant periodic components in the Factor I means profile.

The spectral density plot of factor II and III means (Fig.1.3d) exhibit some peaks in the spectral density plot and several large periodogram ordinates. However, none are statistically significant in the Fisher’s test. The spectral density plot of Factor IV means (Fig.1.3h) has three large periodogram ordinate at 2.58 aa, 3.27 aa 4.9 aa. The 2.58-aa component is not significant. However, the Fisher’s test statistics *g* of the 3.27-aa component is significant, which indicate that there is possible significant periodic component the Factor IV means profile. Finally, Factor V has no statistically significant values according to the Fisher’s test.

In summary, these analyses suggest that the factors I and IV means profiles contain periodicity components which conform to the periodicity of helix secondary structure, although the statistical significance is not strong. Factor I is a multidimensional attribute relating to covariation in polarity, hydrophobicity, accessibility and free energy. Factor IV is related to relative amino acid composition in various proteins, number of codon coding for an amino acid, and amino acid composition (Atchley *et al*., 2005). Other factors have large values around 3.3 to 3.7 but the results do not reach the level of statistical significance in the Fisher’s tests.

Periodicity Analyses of the Factor Score Variances

An entropy profile (Fig.1.2a) is a description of the total site-by-site amino acid diversity without regard to the underlying causal physiochemical attributes.

Consequently, analyses relating the entropy values to the *variances* in factor scores at each site should permit decomposition of the total variability at each amino acid site into its underlying components of attribute variability.

An analysis of variance of the factor score variances has a statistically significant *F*-test value =52.77 (*P*<0.0001) indicating that the explained variation is large relative to unexplained variance. Hence, we can reject the null hypothesis that there is no difference between the total variation of Factor I-V and the error variance. A multiple regression analysis was carried out of the form:

$$\text{Entropy} = \beta_0 + \beta_1(\text{Factor I Var}) + \beta_2(\text{Factor II Var}) + \beta_3(\text{Factor III Var}) + \beta_4(\text{Factor IV Var}) + \beta_5(\text{Factor V Var}) + \varepsilon$$

This analysis gave parameter estimates of β_0 = 0.564 (*P*<.0001), β_1 = 0.470 (*P*=0.052), β_2 = 0.468 (*P*=0.062), β_3 = 0.154 (*P*=0.023), β_4 = 1.263 (*P*< .0001) and β_5 = 0.174 (*P*=0.054). The proportion of the total variation explained by the model has an R^2 = 0.86 meaning that 86% of the variation in entropy values could be explained by these five complex attribute index variables.

The spectral density plot of Factor I variances (Fig.1.3c) has peaks at three periodogram ordinates (2.58 aa, 3.77 aa and 3.27 aa) but none are statistically significant by the Fisher's test. However, analyses of the Factor II variances profile is Fig.1.3e, give a major peak at 3.77 aa, which is statistically significant in the Fisher's test. A follow-up harmonic analysis gives an accurate period estimate as 3.69 aa (R^2=0.285). Similarly, Factor III variances (Fig.1.3g) gave a major peak at 3.77 aa that is also statistically significant in the Fisher's test. The follow-up harmonic analysis gives an accurate period estimate as 3.71 aa (R^2=0.379). The spectral density plot of Factor IV variances (Fig.1.3i) had three peaks at periodogram ordinates at 7 aa, 5.44 aa and 2.13 aa but none are statistically significant. However, the spectral density plot of Factor V variances (Fig.1.3k) had large periodogram ordinates at 3.27 aa, 3.77 aa, and 5.44 aa. The value at 3.77 aa is statistically significant in the Fisher's test.

Thus, Factors II, III and V variances have statistically significant patterns of periodicity. In each instance, the peak occurs at approximately 3.6 – 3.7 aa, which is close to the conventionally accepted value for an α-helix pattern. Factor I and IV variances profiles have no significant periodic components.

Discussion

Herein we describe the application of spectral and multivariate statistical analyses to the patterns of amino acid periodicity in a diverse array of bHLH domain-containing proteins. Our results suggest that these computational techniques can be powerful estimators of important structural features in proteins. Our analyses show that analyzing sequence elements as highly interpretable factor score attribute indices can facilitate other quantitative analyses to explore important evolutionary and structural phenomena in proteins.

These analyses of sequence variability give periodicity estimates that deviate only slightly from the conventionally accepted value of 3.60 aa for an α-helix. Indeed, they fall well within in the known range of 3.40 - 3.91 aa (Kyte, 1995).

What phenomena might be responsible for variable estimates in amino acid periodicity? First, there is variability in sampling. Our analyses are based on a single family of transcription factors containing two short amphipathic α-helices. Thus, we might expect some variability in periodicity among different families of proteins. For example, it has been reported that the number of residues per α-helical turn of a leucine zipper protein is about 3.64 (Thepaut *et al.*, 2004), a value still very similar to that reported here.

Second, more complicated structural phenomena may be at work that adds noise to the estimates. For example, in the basic region of the bHLH protein/DNA complex in Pho4, there are non-regular α-helical turns and the basic region is mostly unfolded relative to residual helical content in the absence of DNA (Cave *et al.,* 2000). Studies on the bHLH-leucine zipper protein Max when uncomplexed with DNA has the first 14 residues of the basic region mostly unfolded. However, the last four residues of the basic region form a persistent helical turn while the loop region is observed to be flexible (Sauve *et al*., 2004). Therefore, the basic region and loop regions may exhibit different periodicity values relative to helix 1 and helix 2. This topic is certainly worthy of further investigation.

The removal of some part of the highly variable loop region (such as done in this report) may distort the long-range periodicity (low-frequency components) evaluation of profiles of multiple alignments. However, removal of part of the loop region has little impact on the short-range periodicity (high-frequency components) as analyzed in this report. Thus, our short-range evaluations in this paper are robust.

It is important to consider the stationarity property of a numeric sequence profile since it can affect the periodicity evaluation. Spectral analysis has a stationary assumption (Warner, 1998), i.e., the mean and variance of the numeric sequence are constant over amino acid sites and structure depends only on the relative position of two observations (Kendall and Ord, 1990). However, different regions of a protein sequence may be subject to different selection pressures during evolutionary divergence. As a consequence, they may display entropy and factor score patterns that are not stationary. In the bHLH case, partitioning the sequence into several short homogeneous regions and then investigating the periodicity for the basic region, Helix 1 and Helix 2 separately could improve the accuracy of the periodicity evaluation. Such findings are expected because structurally and evolutionarily homogeneous regions intend to be more stationary than the entire sequence. Several suggestions have been made for this problem. For example, Warner (1998) has suggested a log transformation of the data might reduce this heterogeneity somewhat. Also, complex demodulation methods (e.g., Bloomfield, 1976) make it possible to describe the change in amplitude of the periodic component across amino acid sites more precisely for nonstationary series.

The ANOVA and multiple regression results described here demonstrate that the overall variation (entropy) in alphabetic amino acids can be significantly related to variation in their major underlying physiochemical attributes. Through studying the influence of these physiochemical components, we are able to understand and explain the causes of the variability patterns observed in protein sequences. Based on the simple model described in this paper, more complex models can be developed that including interaction effects as well as more components.

In summary, our results demonstrate that the major periodic components in the entropy profile and as well as data on several factor score index variances exhibit reflect the classical α-helix periodicity of 3.6 aa. The variances of the factor score for propensity for secondary structure (Factor II), molecular volume (Factor III) and electrostatic charge (Factor V) are significant underlying causal components to site-by-site amino acid diversity in the bHLH domain. Further, the factor score means for polarity and codon composition also contain information related to the helix secondary structure.

These results suggest that periodicity patterns in amino acid diversity reflect significant secondary structure information. Further, entropy as a measure of diversity at each amino acid site can be decomposed into its causal components. These findings should facilitate formal dynamic modeling of both the variability in sequence elements and their underlying causes. Such analyses would provide valuable new information for structural and evolutionary biologists.

It is clear from these analyses that spectral analysis in combination with other powerful statistical procedures can provide valuable information about the periodicities in variability patterns of protein domains. Methods, like those described here, can be used to significantly enhance our understanding of protein variability, structure, function and evolution.

ACKNOWLEDGEMENTS

Thanks to Charles Smith, Andrew Fernandes, Kevin Scott, Andrew Dellinger and the anonymous reviewers for their helpful suggestions. This research was supported by a grant from the National Institutes of Health (GM45344) to WRA.

Fig.1.1

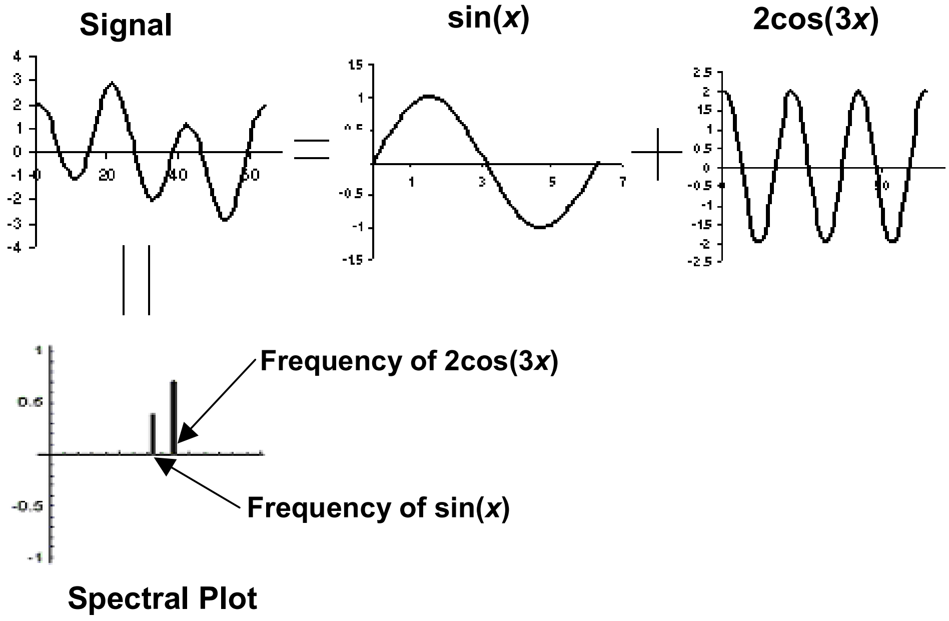
Signal
4
3
2
1
0
-1
-2
-3
-4
20
40
60
sin(x)
1.5
1
0.5
-0.5
-1
-1.5
1
3
5
7
2cos(3x)
2.5
2
1.5
1
0.5
0
-0.5
-1
-1.5
-2
-2.5
50
1
0.5
-0.5
-1
Frequency of 2cos(3x)
Frequency of sin(x)
Spectral Plot

Fig. 1.2

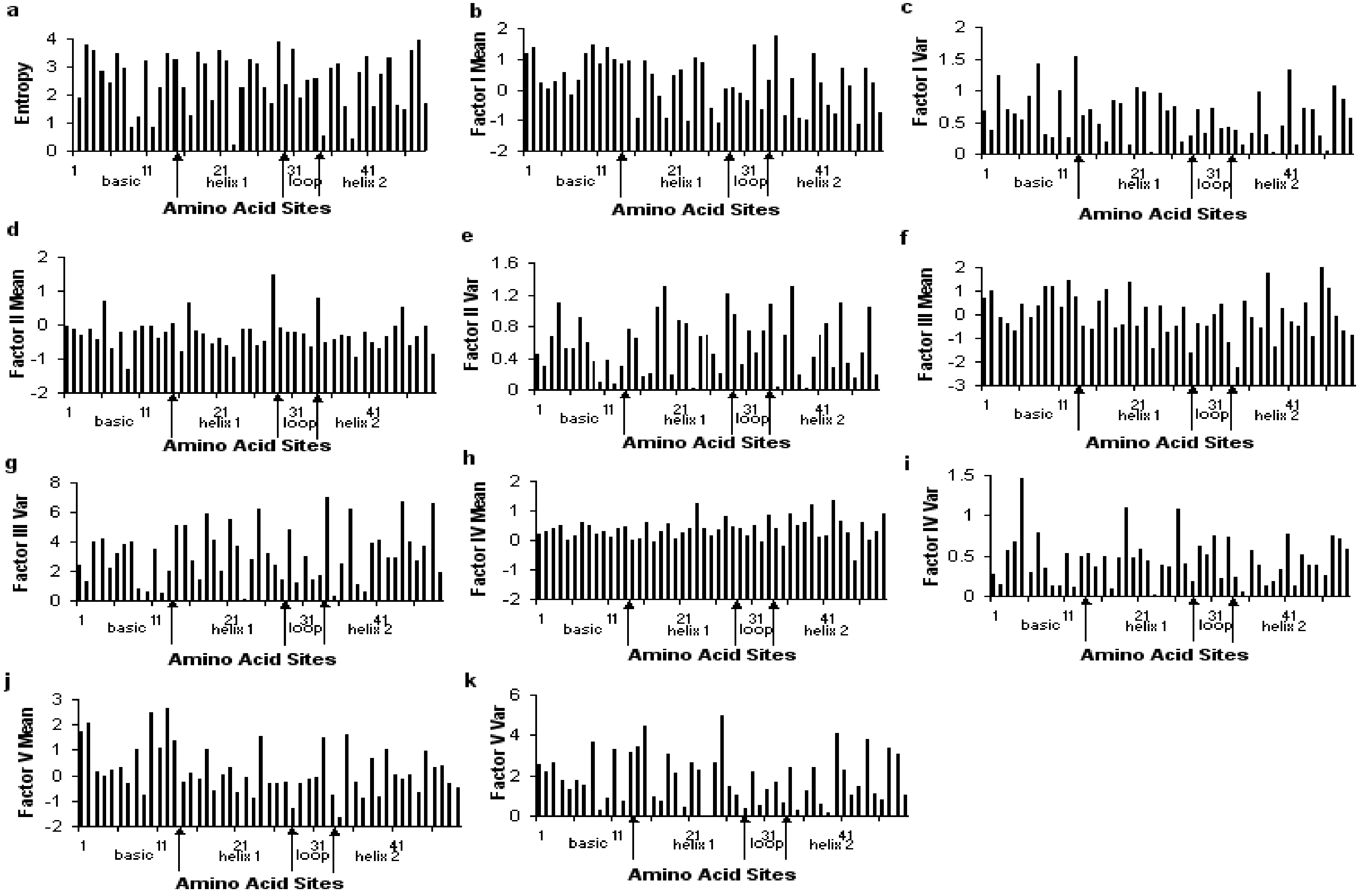

a
Entropy
4
3
2
1
0
1
basic
11
21
helix 1
31
loop
41
helix 2
Amino Acid Sites
b
Factor I Mean
2
1
0
-1
-2
1
basic
11
21
helix 1
31
loop
41
helix 2
Amino Acid Sites
c
Factor I Var
2
1.5
1
0.5
0
1
basic
11
21
helix 1
31
loop
41
helix 2
Amino Acid Sites
d
Factor II Mean
2
1
0
-1
-2
1
basic
11
21
helix 1
31
loop
41
helix 2
Amino Acid Sites
e
Factor II Var
1.6
1.2
0.8
0.4
0
1
basic
11
21
helix 1
31
loop
41
helix 2
Amino Acid Sites
f
Factor III Mean
2
1
0
-1
-2
-3
1
basic
11
21
helix 1
31
loop
41
helix 2
Amino Acid Sites
g
Factor III Var
8
6
4
2
0
1
basic
11
21
helix 1
31
loop
41
helix 2
Amino Acid Sites
h
Factor IV Mean
2
1
0
-1
-2
1
basic
11
21
helix 1
31
loop
41
helix 2
Amino Acid Sites
i
Factor IV Var
1.5
1
0.5
0
1
basic
11
21
helix 1
31
loop
41
helix 2
Amino Acid Sites
j
Factor V Mean
3
2
1
0
-1
-2
1
basic
11
21
helix 1
31
loop
41
helix 2
Amino Acid Sites
k
Factor V Var
6
4
2
0
1
basic
11
21
helix 1
31
loop
41
helix 2
Amino Acid Sites

Fig.1.3

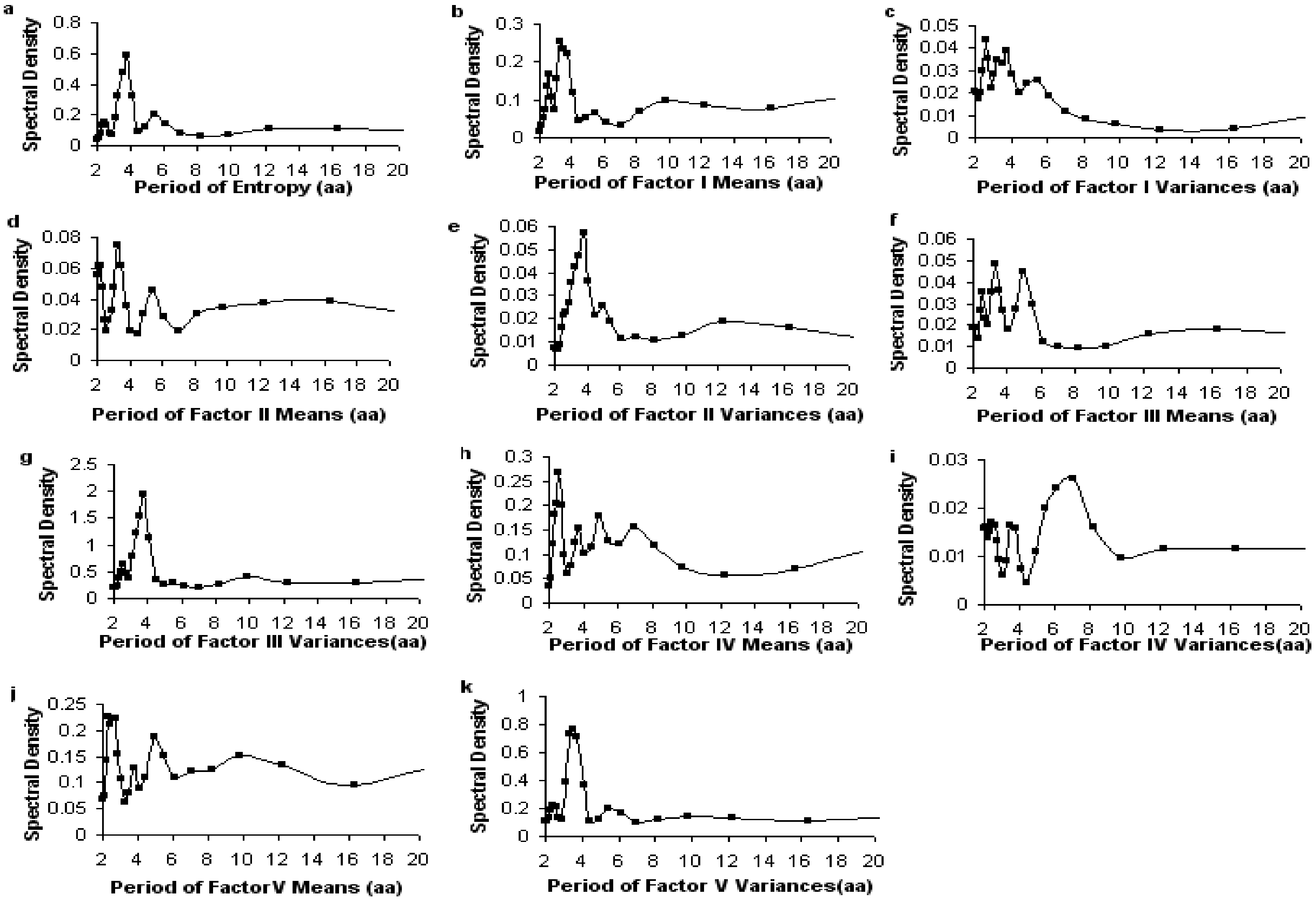
a
Spectral Density
0 0.2 0.4 0.6 0.8
2 4 6 8 10 12 14 16 18 20
Period of Entropy (aa)
b
Spectral Density
0 0.1 0.2 0.3
2 4 6 8 10 12 14 16 18 20
Period of Factor I Means (aa)
c
Spectral Density
0 0.01 0.02 0.03 0.04 0.05
2 4 6 8 10 12 14 16 18 20
Period of Factor I Variances (aa)
d
Spectral Density
0 0.02 0.04 0.06 0.08
2 4 6 8 10 12 14 16 18 20
Period of Factor II Means (aa)
e
Spectral Density
0 0.01 0.02 0.03 0.04 0.05 0.06
2 4 6 8 10 12 14 16 18 20
Period of Factor II Variances (aa)
f
Spectral Density
0 0.01 0.02 0.03 0.04 0.05 0.06
2 4 6 8 10 12 14 16 18 20
Period of Factor III Means (aa)
g
Spectral Density
0 0.5 1 1.5 2 2.5
2 4 6 8 10 12 14 16 18 20
Period of Factor III Variances(aa)
h
Spectral Density
0 0.05 0.1 0.15 0.2 0.25 0.3
2 4 6 8 10 12 14 16 18 20
Period of Factor IV Means (aa)
i
Spectral Density
0 0.01 0.02 0.03
2 4 6 8 10 12 14 16 18 20
Period of Factor IV Variances(aa)
j
Spectral Density
0 0.05 0.1 0.15 0.2 0.25
2 4 6 8 10 12 14 16 18 20
Period of FactorV Means (aa)
k
Spectral Density
0 0.2 0.4 0.6 0.8 1
2 4 6 8 10 12 14 16 18 20
Period of Factor V Variances(aa)

Figure Legends

Fig.1.1 Illustration of the spectral plot of the signal sin(*x*)+2cos(3*x*) produced by Fourier Transformation.

Fig.1.2 Entropy and Factor profiles of bHLH protein domains. (a) Entropy vs. Amino Acid Sites. (b) Factor I Means vs. Amino Acid Sites. (c) Factor I Variance vs. Amino Acid Sites. (d) Factor II Means vs. Amino Acid Sites. (e) Factor II Variances vs. Amino Acid Sites. (f) Factor III Means vs. Amino Acid Sites. (g) Factor III Variance vs. Amino Acid Sites. (h) Factor IV Means vs. Amino Acid Sites. (i) Factor IV Variances vs. Amino Acid Sites. (j) Factor V Means vs. Amino Acid Sites. (k) Factor V Variances vs. Amino Acid Sites.

Fig.1.3 Plots of the spectral density distribution of entropy, Factor score means and variances profiles produced by the Fast Fourier transformation. (a) Spectral density plot of entropy profile. (b) Spectral density plot of Factor I means profile. (c) Spectral density plot of Factor I variances profile. (d) Spectral density plot of Factor II means profile. (e) Spectral density plot of Factor II variances profile. (f) Spectral density plot of Factor III means profile. (g) Spectral density plot of Factor III variances profile. (h) Spectral density plot of Factor IV means profile. (i) Spectral density plot of Factor IV variances profile. (j) Spectral density plot of Factor V means profile. (k) Spectral density plot of Factor V variances profile.

‘

Supplement

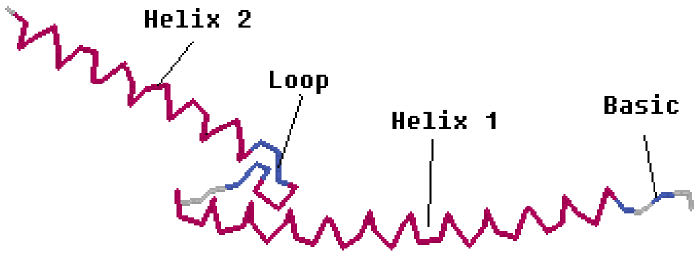

Supplemental Fig.1.1 Three-dimensional Structure of bHLH protein domain of MYC Proto-Oncogene Protein

Supplemental Table 1.1 Five groups of bHLH protein domains

Group	Example Protein	Characteristics
A	Myod	binds to CAGCTG
B	Myc	binds to CACGTG
C	Sim	doesn't bind directly
D	Id	no basic region/doesn't bind
E	Hes	may bind CACGCG or CACGAG

White Noise Tests

In the context of spectral analysis, white noise may be defined more formally as an equal mixture of all the frequencies. In other words, there is no individual periodic component that can explain a larger share of the variance over other periodic components (Warner,1996). Instead of showing peaks in the spectrum of the signal (e.g. the data series), white noise shows a flat straight line due the same contribution of individual periodic components.

Therefore, two white noise tests, Fisher's Kappa tests and Bartlett's Kolmogorov-Smirnov (BKS) are conducted (SAS, 1992) to analyze the bHLH protein domain. The results are shown in Table 2. Although these statistical tests can provide statistical information about periodicity patterns, we should be cautious when applying the results to explain the numeric sequence profile and equating statistical and biological significance. For example, even if a periodic component is not statistically significant by the Fisher's test, it still may have some biological meaning. Even if a numeric sequence profile is assumed to be white noise, the corresponding amino acid sequence may still contain biological information about structure, function and evolution.

The entropy and Factor III variances profiles are rejected as white noise. Factor II and Factor V variances profiles are also susceptible as white noise because both *p*-values are less than 0.1. Other profiles are not rejected as white noise in both statistical tests.

Supplemental Table 1.2 Results of white noise tests for the entropy, factor score means/ variances profiles.

White Noise Tests Profile	**Fisher's Kappa Test Statistics**	**Bartlett's Kolmogorov-Smirnov (BKS) Test Statistics**
Entropy	7.38 (*p*<0.01)	0.217 (*p* = 0.21)
Factor I Means	4.70 (*p*>0.1)	0.16 (*p*=0.55)
Factor I Variances	3.27 (*p*>0.1)	0.18 (*p* = 0.38)
Factor II Means	3.61 (*p*>0.1)	0.15 (*p*=0.63)
Factor II Variances	5.24 (0.05<*p*<0.1)	0.17 (*p* = 0.47)
Factor III Means	3.70 (*p*>0.1)	0.11 (*p*=0.92)
Factor III Variances	7.65 (*p*<0.01)	0.27 (*p* = 0.06)
Factor IV Means	4.03 (*p*>0.1)	0.18 (*p*=0.43)
Factor IV Variances	3.46 (*p*>0.1)	0.11 (*p* = 0.93)
Factor V Means	3.01 (*p*>0.1)	0.13 (*p*=0.85)
Factor V Variances	5.42 (0.05<*p*<0.1)	0.24 (*p* = 0.12)

Supplemental Table 1.3 Summary of the fundamental periods of the entropy profiles for the whole sequence, Basic region, Helix 1 and Helix 2. The percentage of variance indicates the percentage of total variance contributed by the periodic component with major periods.

Entropy Profile	Fundamental Period	Model	R^2
Whole Domain	3.68	$\mathrm{Yt} = 2.497\text{-}0.2915\sin(\frac{2\pi}{T}t) + 0.8963\cos(\frac{2\pi}{T}t)$ $T = 3.68 \quad \mathrm{t} = 1,2,...49$	0.457
Basic Region	3.56	$\mathrm{Yt} = 2.5238{+}0.1713\sin(\frac{2\pi}{T}t) + 0.9431\cos(\frac{2\pi}{T}t)$ $T = 3.56 \quad \mathrm{t} = 1,2,...13$	0.463
Helix 1	3.59	$\mathrm{Yt} = 2.5423 + 0.3335\sin(\frac{2\pi}{T}t) + 0.9567\cos(\frac{2\pi}{T}t)$ $T = 3.59 \quad \mathrm{t} = 14,15,...28$	0.530
Helix 2	3.59	$\mathrm{Yt} = 2.3744{+}1.3057\sin(\frac{2\pi}{T}t){+}0.0028\cos(\frac{2\pi}{T}t)$ $T = 3.59 \quad \mathrm{t} = 35,36,...49$	0.777

Spectral Density Plots Produced by Burg Methods

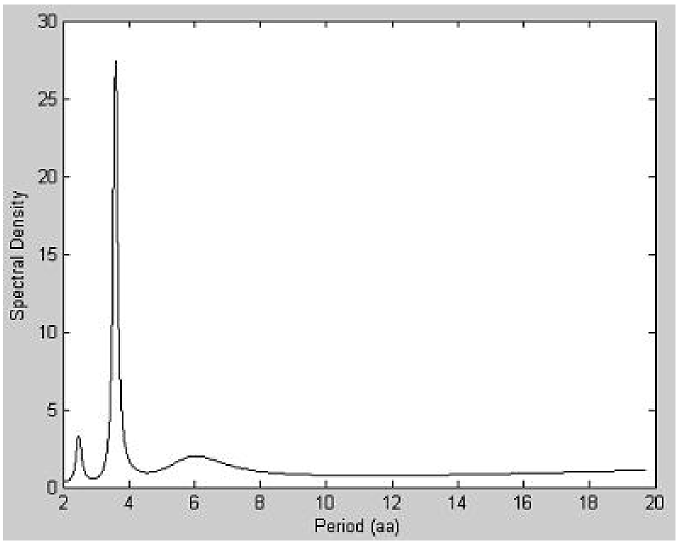

Supplemental Fig.1.2 Spectral density plot of entropy profile produced by Burg method.

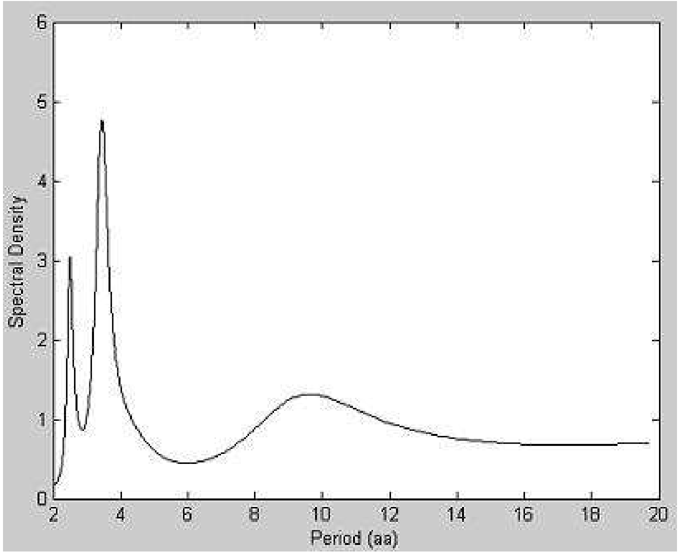

Supplemental Fig.1.3 Spectral density plot of Factor I means profile produced by Burg method.

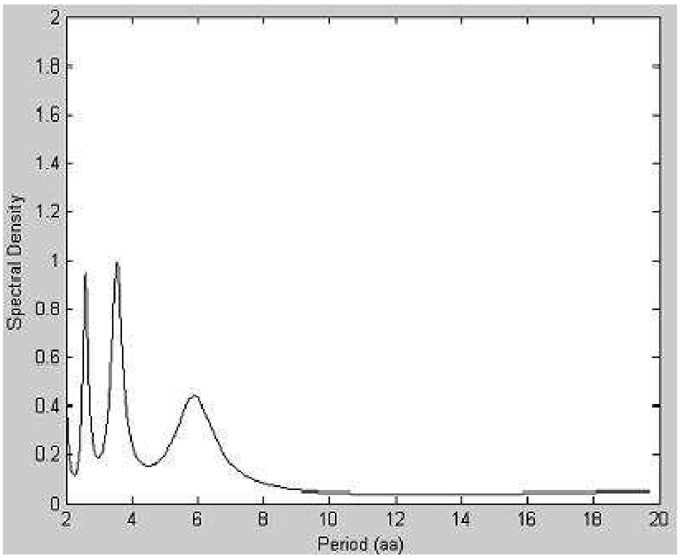

Supplemental Fig.1.4 Spectral density plot of Factor I variances profile produced by Burg method.

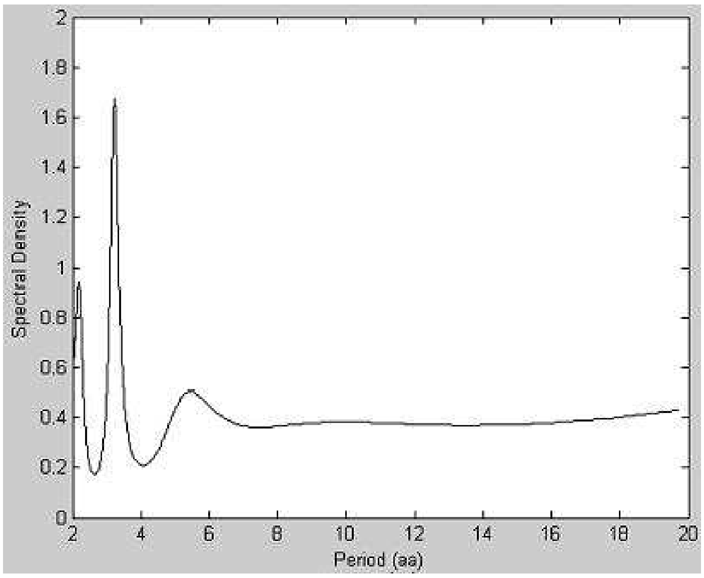

Supplemental Fig.1.5 Spectral density plot of Factor II means profile produced by Burg method.

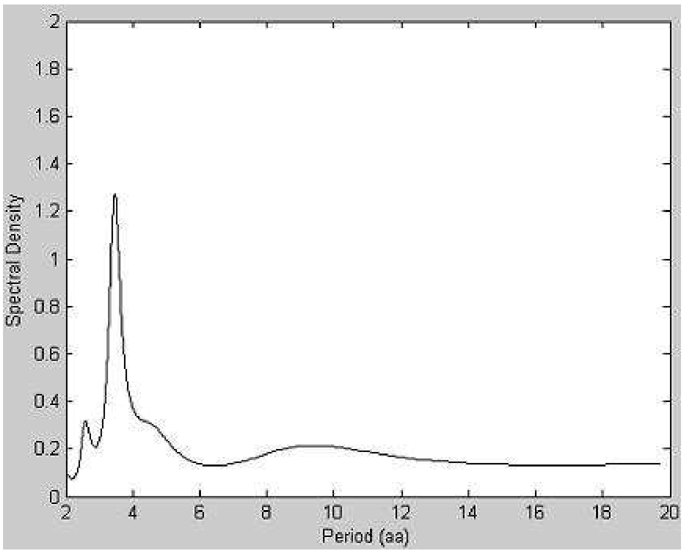

Supplemental Fig.1.6 Spectral density plot of Factor II variances profile produced by Burg method.

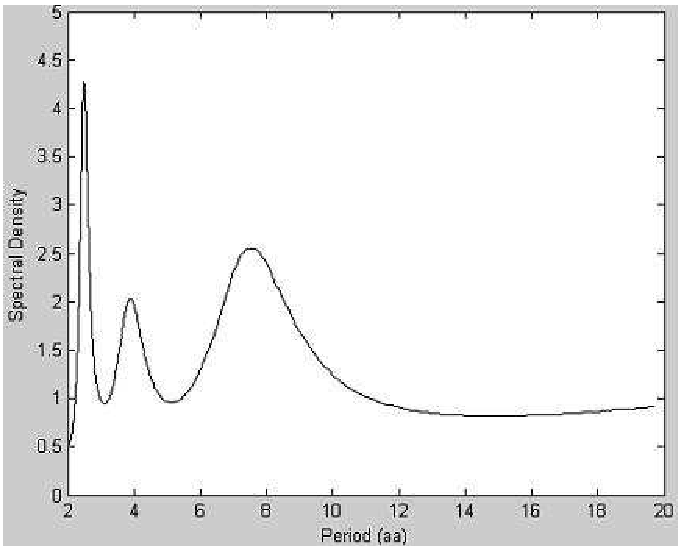

Supplemental Fig.1.7 Spectral density plot of Factor III means profile produced by Burg method.

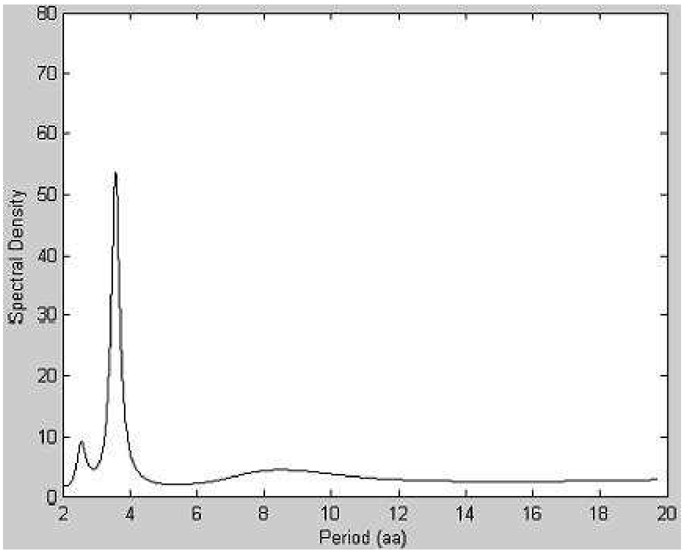

Supplemental Fig.1.8 Spectral density plot of Factor III variances profile produced by Burg method.

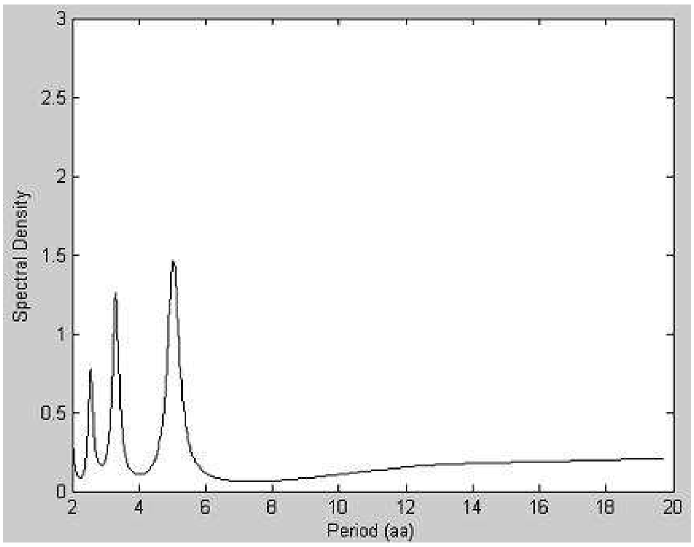

Supplemental Fig.1.9 Spectral density plot of Factor IV means profile produced by Burg method.

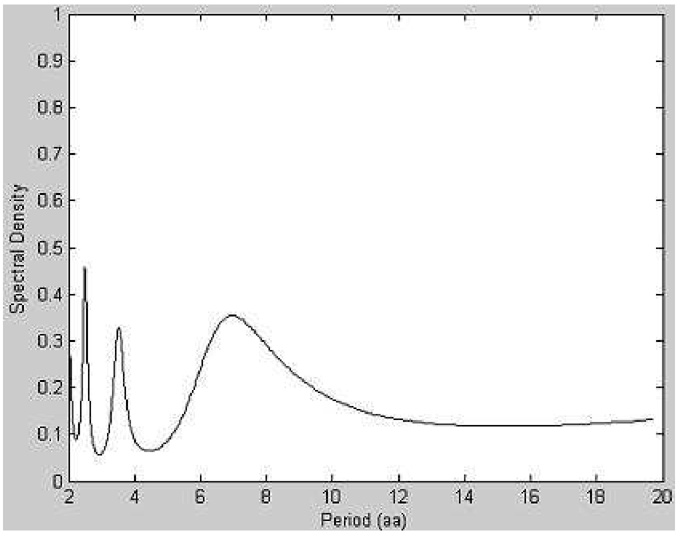

Supplemental Fig.1.10 Spectral density plot of Factor IV variances profile produced by Burg method.

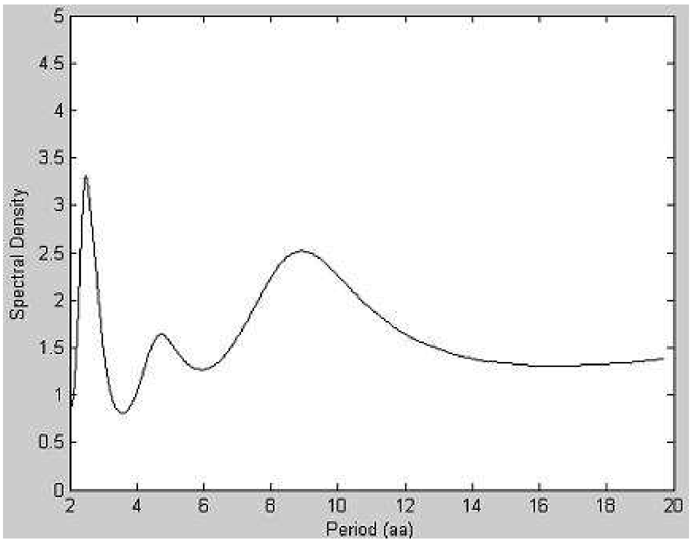

Supplemental Fig.1.11 Spectral density plot of Factor V means profile produced by Burg method.

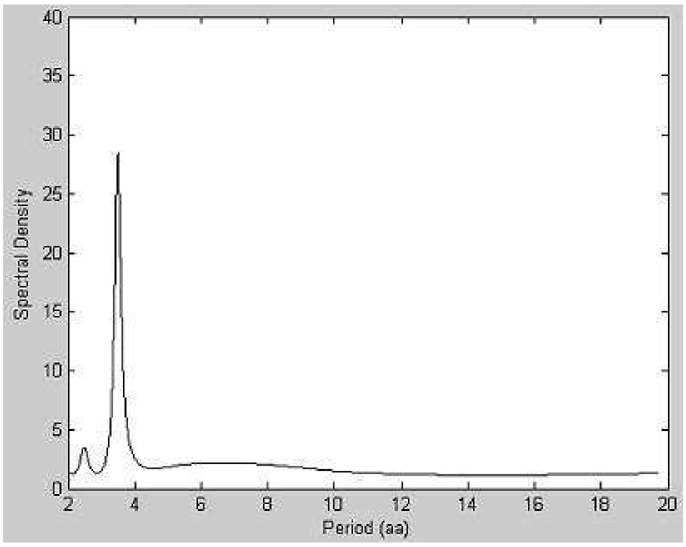

Supplemental Fig.1.12 Spectral density plot of Factor V variances profile produced by Burg method.

Supplemental Plots of Analyses on Entropy profile

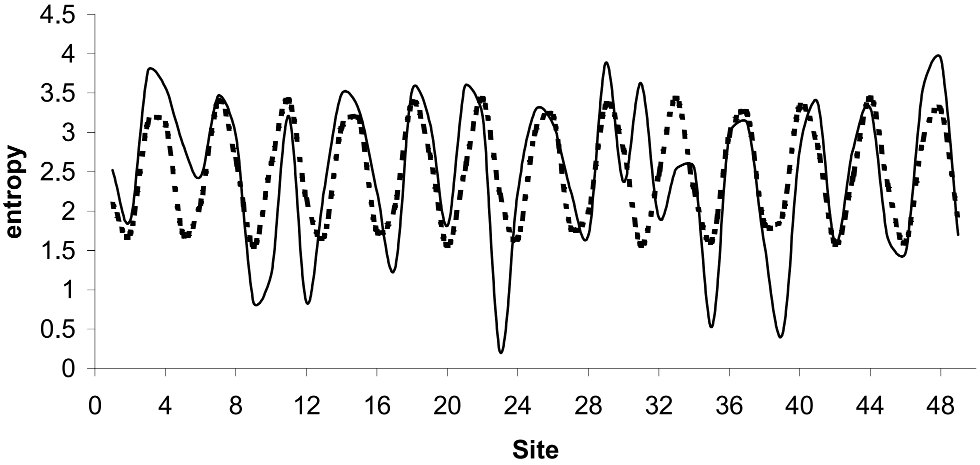

Supplemental Fig.1.13 Plot of the observed entropy profile (smooth curve) and the predicted entropy profile (dotted curve) with a period of 3.68 aa.

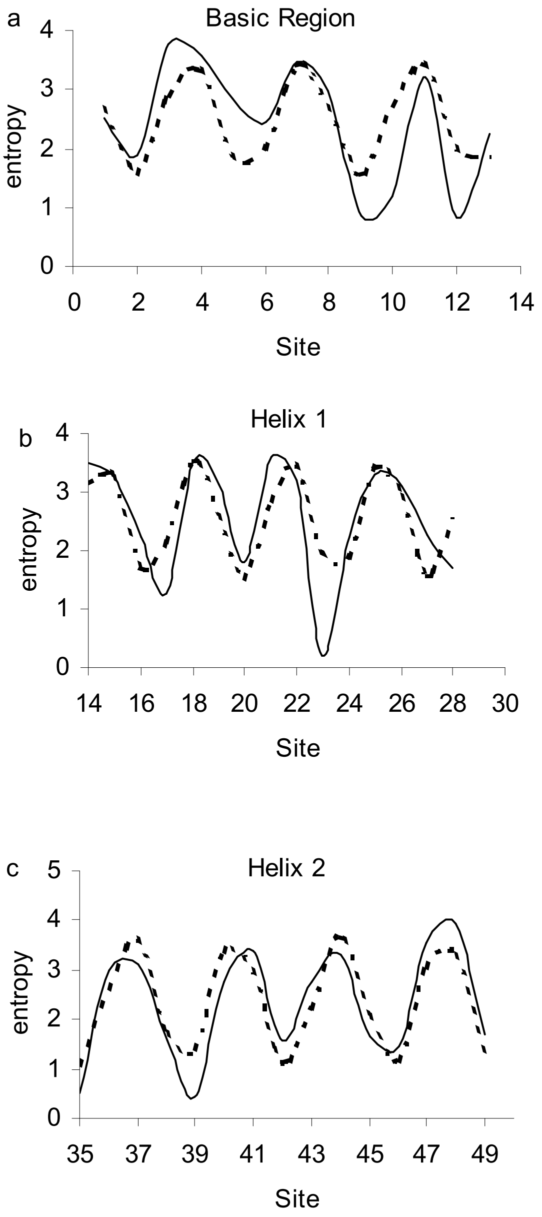

Supplemental Fig.1.14 Plot of the observed and predicted entropy profiles for each region. (a) Plot of the observed entropy profile (smooth curve) and the predicted entropy profile (dotted curve) with a period of 3.56 aa for the Basic region. (b) Plot of the observed entropy profile (smooth curve) and the predicted entropy profile (dotted curve) with a period of 3.59 aa for the Helix 1 region. (c) Plot of the observed entropy profile (smooth curve) and the predicted entropy profile (dotted curve) with a period of 3.59 aa for the Helix 2 region.

Chapter 2

Application of Complex Demodulation on bZIP and bHLH-PAS Protein Domains

by

Zhi Wang[1,*] , William R. Atchley[1,2], Charles E. Smith[1]

[1]Graduate Program In Biomathematics and [2]Department Of Genetics and Center For Computational Biology, North Carolina State University, Raleigh, NC 27695-7614, USA

Keyword: periodicity, complex demodulation, functional region

[*] To whom correspondence should be addressed

[*] CONTACT: zwang2@ ncsu.edu

ABSTRACT

Proteins are built with molecular building blocks such as α-helix, *β*-sheet, loop region and else, which is an economic way of constructing complex molecules. Periodicity analysis of protein sequences has allowed us to obtain meaningful information of their structure, function and evolution. In this work, complex demodulation (CDM) is introduced to detect functional regions in protein sequences data. We analyzed bZIP and bHLH-PAS protein domains and found that complex demodulation can provide insightful information of changing amplitudes of periodic components in protein sequences. Furthermore, it is found that the local amplitude minimum or local amplitude maximum of the 3.6-aa periodic component is associated with protein structural or functional information due to the observation that they are mainly located in the boundary area of two structural or functional regions.

Introduction

Recent developments in computational methodology have provided mechanisms to statistically transform alphabetic sequence information into biologically meaningfully arrays of numerical values (Atchley *et al*., 2005). Using a multivariate statistical approach, these authors generated five multidimensional indices (factors) of amino acid attributes that reflect polarity, secondary structure, molecular volume, codon diversity, and electrostatic charge of sequences. This advance will make possible a number of statistical and mathematical analyses that will facilitate our understanding of the structure and function of biological sequence data.

For example, it has been suggested that periodicity of a sequence can be evaluated by Fourier transformation or spectral analysis (Pasquier *et al*., 1998). Periodicity of biological sequences is an important indicator of protein structure and DNA folding (Herzel *et al*., 1999; Schieg and Herzel, 2004). However, the Fourier analysis or spectral analysis is not useful in assessing the changes in cycle parameters, such as amplitude and phase of the periodic components over the sequence.

Recently, the technique of complex demodulation (CDM) has been introduced to provide a continuous assessment of the periodic amplitude and thereby identify regions of change in structural and functional aspects of biological sequences. Complex demodulation has been widely used in many fields such as physiology, psychology and oceanography research (Hayano *et al*., 1993; Lipsitz *et al*., 1998;

Babkoff *et al.*, 1991; Rutherford and D'Hondt 2000). However, there are obviously no applications of CDM procedures in computational biology and bioinformatics.

Therefore, this paper is to illustrate the application of CDM method on protein sequences with the case study of bZIP and bHLH-PAS protein domains. This paper is also an exploratory work to ascertain if the amplitude of a certain periodic component of a protein sequence has biological information. The bZIP and bHLH-PAS proteins are selected because of the complexity of their function and structure, which can represent the complex characteristics of biological signals.

In this article, we show that CDM can describe the changing amplitude of a certain periodic component. The amplitude pattern of the 3.6-aa periodic component is closely associated with the secondary structure of the protein sequences. It is found that the amino acid sites with local amplitude maximums and local amplitude minimums mostly occur at the boundaries of helices and strands. This strongly suggests that CDM method is a new computational tool of helping us to understand biological sequences. There are several methods available to predict the regular secondary structure, however, the number of correctly predicted α-helix start positions was just 38% (Wilson, 2004). This research should trigger more interests in CDM and more exploration works to apply CDM method to analyze the biological sequences.

Methods

Principle of Complex Demodulation

Not every "periodic" series has simple representation in terms of cosine or sine functions. A perturbed periodic component may have changing amplitude and changing phase. Therefore, the goal of complex demodulation is to quantify the amplitude and phase as a function of time. The amplitude and phase are determined by the data in the neighborhood of *t*, rather than by the whole series. The principle of complex demodulation has been well documented by Bloomfield (1976) so that it is briefly described here before showing the case study results on the bZIP and bHLH-PAS proteins. Given the fundamental period of a biological sequence, CDM can extract approximations of the changing amplitude and changing phase as a function of the position of nucleotides or amino acid residues. If numerical series data x_t of a biological sequence is known to include a component oscillating around a frequency of λ (the amplitude and the phase may varies), then x_t can be written as

$$X_t = A_t \cos(\lambda t + \phi_t) + z_t \qquad (1)$$

where A_t and $Ø_t$ are the changing amplitude and phase of the periodic component and z_t is residue including all other components and noises. Fig.2.1 is a good illustration of power spectrum analysis and complex demodulation of simulated data (Hayano *et al*., 1993). It is obvious from this figure that CDM is able to extract approximations of A_t (amplitude) as a function of time. $Ø_t$ can be also represented as a function of time, but this phase plot hasn't been shown here.

In factor, the real-valued time series (1) can be regarded as complex-valued series and hereby can be easily processed in computation. With the Euler relation $\cos\lambda + i\sin\lambda = \exp(i\lambda)$, the time series X_t in (1) is converted to its complex analogue

$$X_t = \frac{1}{2}A_t\{\exp[i(\lambda t + \phi_t)] + \exp[-i(\lambda t + \phi_t)]\} + z_t \qquad (2)$$

where *i* is a complex number and i^2= -1.

We then obtain a new signal y_t by shifting all the frequencies in X_t by –*λ*. This procedure is called CDM and y_t is expressed as

$$y_t = 2x_t \exp[-i\lambda t] \qquad (3)$$

Inserting equation (2) into (3), equation (3) then becomes

$$y_t = A_t \exp(i\phi_t) + A_t \exp[-i(2\lambda t + \phi_t)] + 2z_t \exp(-i\lambda t) \qquad (4)$$

The first item of equation (4) is smooth (the frequency is around zero), the second term oscillates at a frequency of -2*λ* and the third item is assumed to contain no component around the zero frequency from the definition of z_t. Therefore, when we let Y_t be the signal obtained by passing y_t through a low-pass filter, we would obtain Y_t in complex version as

$$Y_t = A_t \exp(i\phi_t) \qquad (5)$$

Here Y_t is represented by a set of complex numbers in terms of its magnitude and phase, A_t and $Ø_t$. The instantaneous amplitude of the periodic component is defined as

$$A_t = |Y_t| = \sqrt{Y_t Y_t^*} \qquad (6)$$

where Y_t^* is the complex conjugate of Y_t . The phase $Ø_t$ can be then caculated.

The FORTRAN program of CDM was listed by Bloomfield (1976). From a frequency-domain perspective, the power spectrum of x_t has a peak around a frequency of λ. As the result of CDM, the peak is moved leftward to around zero frequency in the power spectrum of y_t (in the PSD-frequency plot). For example in Fig. 2.1, if CDM is applied to the low-frequency periodic component A with a frequency around 0.09 HZ, then the Low-frequency peak will move leftward to around zero frequency. The peaks of all other components in x_t, if any, are also moved leftward, those at an original frequency above λ do not reach zero frequency, and those below λ move into the negative part of the frequency axis.

Thus, is is desirable for a low-pass filter to exclude all components except the zero-frequency component and then the amplitude can be determined. The low-pass filter is designed according to the least squares filter design method presented by Bloomfield (1976). The transfer function of the ideal low-pass filter is

$$H(\omega) = \begin{cases} 1 & if\, 0 \le \omega \le \omega_c \\ 0 & if\, \omega_c < \omega \le \pi \end{cases} \qquad (7)$$

where ω_c is the cutoff frequency. The Fourier coefficients of $H(\omega)$ are

$$h_u = \frac{\sin u\omega_c}{\pi u} \qquad u \ge 1 \quad \text{and} \quad h_0 = \frac{\omega_c}{\pi} \qquad (8)$$

We have to construct a smoothing function to approximate the ideal low-pass filter in computation. Convergence factors are used to accelerate the convergence of Fourier series and achieve better approximation of the transfer function *H*(*ω*) in equation (7). According to Bloomfield, the smoothed function approximating *H*(*ω*) is

$$\tilde{H}_s(\omega) = h_0 + 2\sum_{u=1}^{s} h_u \frac{\sin u\delta/2}{u\delta/2}\cos u\omega \quad (9)$$

The multiplier $\frac{\sin 2\pi u/(2s+1)}{2\pi u/(2s+1)}$ is an example of convergence factor. The smoothed transfer function, which are initially 1 and decay to smoothly 0, are a smooth approximation to the ideal filter *H*(*ω*). Fig.2.2 shows the smoothed transfer functions for *s*=5 (an 11-term filter) and *s*=20 (a 41-term filter), and the ideal transfer function.

It is important to note that the amplitudes obtained with the use of complex demodulation are relative rather than absolute measures. This is due to several factors, including the following: (i) the signal is not exactly sinusoidal. And (ii) the absolute measures of the amplitude represents the sum of high and low frequency periodic components, however, complex demodulation separates out the amplitudes at each frequency.

Computational Procedures

First, we transform the biological sequences into numeric values. In our case study, a protein sequence is transformed into a numeric array of factor scores

(Atchley *et al*., 2005). The variability of protein multiple alignments is measures as a numeric array of entropy values.

Second, spectral analysis is conducted to produce power spectral density (PSD) plot (as shown in Fig.2.1). Through examining the PSD plot, certain periodic component of interests can be selected for the following CDM procedure.

Third, given a periodic component of interests, CDM is applied to produce a plot of instantaneous amplitude and phase of the periodic component of interests as a function of amino acid sites.

Data Types

The data utilized in this study are basic region-leucine zipper (bZIP) protein domain and basic region-helix-loop-helix-PAS (bHLH-PAS) protein domain. The bZIP proteins and bHLH-PAS are both very important transcription factors. bZIP proteins contain a basic region mediating sequence-specific DNA-binding, followed by a leucine zipper region, which is required for dimerization (Podust *et al*., 2001). Both the basic region and the leucine zipper region have a helix form. Binding to DNA induces a coil-to-helix transition of the basic DNA-binding region. The leucine zipper region exhibits a stable helix form. bZIP domain is one of the simplest types of DNA-binding domains. However, the bZIP transcription factors are capable of recognizing a diverse range of DNA sequences and regulate the gene transcription. The collection of 321 bZIP protein sequences (clad bzip_2) was retrieved from the database Pfam (Dec,2004).

The second group of proteins to be analyzed are the bHLH-PAS proteins. They are a family of sensor proteins involved in signal transduction in a wide range of organisms. The bHLH-PAS domains contain a structurally conserved α/β-fold. There are basic region-helix-loop-helix motif, PAS-1 and PAS-2 motifs in the domain. The illustration of structure-based sequence alignment and the structure of bHLH-PAS domains can be found in Supplemental Fig.2.2 -2.3. Both PAS-1 and PAS-2 motifs contain a five-stranded antiparallel *β*-sheet with one face flanked by several α –helices (Yildiz *et al*., 2005). The PAS-1 and PAS-2 motifs are connected by a short linker.

The choice of bZIP and bHLH-PAS proteins is based on their structural and functional attributes. Since there are subtle differences among different regions of the sequences, it is intriguing to distinguish the differences between these various regions and to explore a novel approach to identifying the boundary of each region. It is hypothesized that CDM can distinguish the subtle differences among the structural and functional regions of sequences with a similar helix conformation. If CDM is able to distinguish the subtle differences, it is expected to work better for regions of sequences have more structural and functional differences. bHLH-PAS contains complex α/β-fold which provides us with a complicated data set to examine the CDM procedure.

Results

bZIP Protein Domain

An entropy profile was calculated (Fig.2.3) based on the method described by

Atchley *et al.* (2000). Such a profile is a numeric representation of the residue diversity at each amino acid site in a set of aligned proteins. Large entropy values represent high variability for that site while small values represents low variability. In our aligned sequence database, the basic region in bZIP proteins ranges from residue 1 to 27 while the leucine zipper region extends from residue 28 to 55. There are interesting oscillations of the entropy values and the periodic component was identified by spectral analysis (Bloomfield, 1976).

A spectral density plot (Fig.2.4) for this entropy profile was produced by the spectral analysis method-Fast Fourier Transformation (Bloomfield, 1976) using SAS software (PROC SPECTRA). The peak at around 3.6 aa indicates that there is a major significant periodic component of at that point in the entropy profile. Increases of spectral density in the period range from 13.75aa to 56 aa indicate that there is also low-frequency periodic component, whose period estimate is much larger. The largest period estimate can be the length of the whole numeric sequence, but such estimate is meaningless.

We focus on the high-frequency periodic component at around 3.6aa that conforms to the average 3.6 aa per turn for an ideal α-helix. The CDM procedure was then used to analyze the amplitude of the 3.6-period component as a function of amino acid sites. We are particularly interested in locating the boundary between the basic region and the leucine zipper region.

The amplitude of the periodic component at 3.6 aa vs. residue is plotted in the dotted line in Fig.2.3. We found there is amplitude decrease in the boundary region between the basic and leucine zipper regions. The entropy amplitude at residue 27 achieved a local minimum. Structural studies indicate that residue 27 is the last residue of the basic region and the ZIP region starts at residue 28 (Pfam, 2005)

These results indicate that the entropy amplitudes of residues located in the end of the basic region and near the start of the ZIP region are significantly smaller than the average values (*t*-test: *p*-value<0.05). The maximal entropy amplitude occurs at residue 42. These latter findings indicate that some residues in leucine zipper region are highly conserved while others are highly variable. The latter results in large amplitude which is reflected by large fluctuations in the entropy values.

These findings suggest that the existence of local minimum entropy amplitude identifies the boundary of specific structural or functional regions. It is interesting that the entropy amplitude at residue 4 has global minimal amplitude and the amplitude increases beyond residue 4. This observation suggests a functional and structural difference of these residues that warrants further investigations.

Next, we investigate the Factor I profile (Atchley *et al*., 2005) of the bZIP domain of the well-studied transcription factor C-fos shown in Fig.2.5. The sequence of the domain (primary accession number: P01100; secondary accession number: P18849, Glover, 1995) is :

139-KRRIRRERNKMAAAKCRNRRREL|TDTLQAETDQLEDEKSALQTE IANLLKEKEKLEFI LAAH-200
Basic Region | Leucine Zipper

The spectral plot of c-fos factor I profile does not reveal a significant periodic component at around 3.6 aa (Fig.2.6). However, implemented the CMD method assuming that there is a periodic component of 3.6 aa and we obtain the amplitude of it (dotted curve in Fig.2.5).

Based on the known structure of the c-fos protein (Glover, 1995), the leucine zipper region starts at residue 162 (labeled in Fig.2.5). However, the amplitude of the 3.6-aa periodic component of Factor I at residue 162 is not significantly different from the average (*t*-test, *p*>0.05) and indeed the local minimum is not at residue 162. However, the minimal amplitude of factor I occurs at residue 164, which is close to the leucine zipper starting residue of 162. This result suggests that the CDM method is somewhat robust to predict the start point of a new structural or functional region, even if there is no significant 3.6-aa periodic component of Factor I. The deviation of the leucine zipper start residue from the residue with a minimal amplitude is possibly related to the absence of a statistical significant 3.6-aa periodic component of Factor I. This observation provides us with an interesting topic that may trigger further investigation.

PAS Protein Domain

Within the bHLH/PAS proteins the PAS region is involved in protein dimerization with another protein of the same family (Ponting and Aravind, 1997; Hefti *et al*., 2004; Zhulin *et al*., 1997). It has also been associated with light reception, light regulation and circadian rhythm regulators (clock). In bacteria, the PAS repeat is usually associated with the input domain of a histidine kinase, or a sensor protein that regulates a histidine kinase. 77 bHLH-PAS protein domains were obtained from PFAM database (version 17.0 May, 2005). The entropy profile of 77 bHLH-PAS domains is shown in Fig.2.7.

The spectral density plot of the entropy profile of bHLH-PAS protein domains is given in Fig.2.8. Only short-range periodicity (i.e. high-frequency components) is shown in Fig.2.8. There are peaks located in the 3.40-3.91 aa range that signal the existence of an α-helix (Kyte, 1995). Therefore, CMD method is conducted to produce the amplitude of the 3.6-aa periodic component as a function of amino acid site (in dotted curve in Fig. 2.7).

Further, we investigate the Factor I profile of a well-known bHLH-PAS protein Arnt_human protein (p27540/ gi:114163) , whose secondary structure has been determined (Hoffman *et al.*, 1991). It is a 789 aa-length protein containing bHLH/PAS1/PAS2 domains (Basic region: 90..102 ; Helix-loop-helix region: 103..143; PAS 1 domain: 161..235; PAS 2 domain 349..419). Regions 1-50 and 468-789 are removed because of they are included in the bHLH/PAS domain. The estimated secondary structure of the Arnt protein is obtained via Prediction protein web server.

The spectral density plot of the Factor I profile of Arnt protein has been produced in Fig.2.9. There are some peaks located in the 3.40-3.91 aa range which signals the existence of α-helix, especially there is a large peak at around 3.6 aa (Kyte, 1995).

The Factor I profile of Arnt protein domain is show as histogram in Fig.2.10. The CMD method produces the amplitude as a function of amino acid sites for the 3.6-aa periodic component (curve in Fig.2.10).

Many local amplitude minimums have implication for the boundary of the α-helix regions or beta-sheets (Table 2.1). Local minimum residue 102 is the ending residue of the basic region of the bHLH conserved domain. Local minimum 158 is close to the beginning residue 161 of PAS domain 1 ranging from residue 161 to 235. Local minimum 344 is close to the beginning residue 349 of PAS domain 2 ranging from residue 349 to 419.

Most local amplitude maximums have implication the boundary of the α-helix regions or beta-sheets (Table 2.1). The results are: Local maximum residue 143 is the ending residue of the 2nd helix of the HLH region. Local maximum residue 171 is the ending residue of an α-helix; local maximum residue 291 is close to the ending residue of a predicted α-helix; local maximum residue 273 is located between two beta-sheets; local maximum residue 313 is close to the ending residue of a predicted beta-sheet; local maximum residue 334 is the beginning residue of a predicted beta-sheet; local maximum residue 355 is the beginning residue of a predicted beta-sheet; local maximum residue 397 is the 2nd beginning residue of a predicted beta-sheet. The only exceptions are: local maximum residue 220 is located within a predicted α-helix region; local maximum residue 413 is located in a predicted beta–sheet region.

Discussion

From the case study of well-known protein sequences of bZIP and bHLH-PAS proteins, the amplitude of certain periodic component is proved to contain meaningful biological information. The complex demodulation procedure is able to quantify the amplitude and phase of periodic components of protein sequences. It is the first time to introduce and illustrate the applications of complex demodulation on biological sequences. The analyses reveal that the minimums or maximums of amplitudes of the 3.6-aa periodic component of protein profiles (i.e. entropy and factor I profiles) are predictors of the boundaries of helices secondary structures. The results in the paper should trigger the scientific interests of investigating the application of the CDM method on computational biology and bioinformatics. Possiblely the analyses of the amplitudes or phased of periodic components through the CDM method could reveal very important functional and structural information. Also it may be used to improve the accuracy of the prediction for N-termini of α-helices because the current prediction accuracy is just 38% (Wilson, 2004).

Hayano (1993) has address three concerns of the CDM performance. 1) Is the resolution sufficient enough to distinguish between the LF and HF components? 2) Is the estimation of amplitude robust against alterations in the frequencies of the components? 3) What is the upper limit of rapid changes in amplitude that can be detected by the analysis? Hayano examined a cosine wave that had a linearly increasing frequency from 0 to 0.5 Hz during 1,000 s and had a constant amplitude of 50. CDM calculated the Low-frequency and High-frequency amplitude only when the instantaneous frequency was between 0.055 and 0.125 Hz and between 0.175 and 0.445 Hz, respectively. Hayano reported that the CDM can not only distinguish the Low-frequency and High-frequency amplitudes but also exclude the influence of the DC trends (those frequency<0.022HZ) on the Low-frequency amplitude. To examine the alterations in the frequencies of the component, Hayano simulated a signal by adding two sine waves whose frequencies were fluctuating between 0.06 and 0.12 Hz and between 0.18 and 0.44 Hz. The Low-frequency and High-frequency amplitude are then calculated by CDM. The results showed slight fluctuations of only 1.6 and 4.5%, whereas the power spectral plot showed wide-based multiple peaks reflecting the fluctuating frequencies of the components. These results indicate that the amplitude estimated by CDM is sufficiently robust against the alterations in the frequency of the signal. Further, the simulation of Hayano suggests that CDM provides a reliable estimate of amplitude when the frequency of amplitude fluctuations was below 0.034 Hz for the LF component and below at least 0.040 Hz for the HF component.

During the filtering procedure, the input signal will be truncated at both ends because the use of the low-pass filter is analogous to the use of a data window. In the practice of analyzing series, the standard way is to extend the input signal with arbitrary numeric sequences like 0000000 or 1111111111 so that the original data is not truncated. In this research, I find that this may be influence of the arbitrary numeric sequences on the estimation of amplitudes. Therefore, the moving average can be considered as an alternative of the arbitrary numeric sequences. Also in this research, the phase plot produced by the CDM method is not included because Hayano (1993) has stated that the phase alternation (i.e. the frequency alternation) has little influence on the amplitude estimation. The results in this research are based on case studies on the bZIP and bHLH-PAS protein domains. It is expected that more representative protein sequences are examined with this CDM method.

All in all, the CDM method is a promising computational procedure to quantify the amplitude of the numeric profiles of protein sequences, which contains a lot of unknown biological information and signals. A lot follow-up applications of the CDM methods are expected to promote our understanding of the complex protein sequences and structures.

ACKNOWLEDGEMENTS

Thanks for helpful suggestions from Andrew Fernandes. This research was supported by a grant from the National Institutes of Health (GM45344) to WRA.

Figure

Fig. 2.1

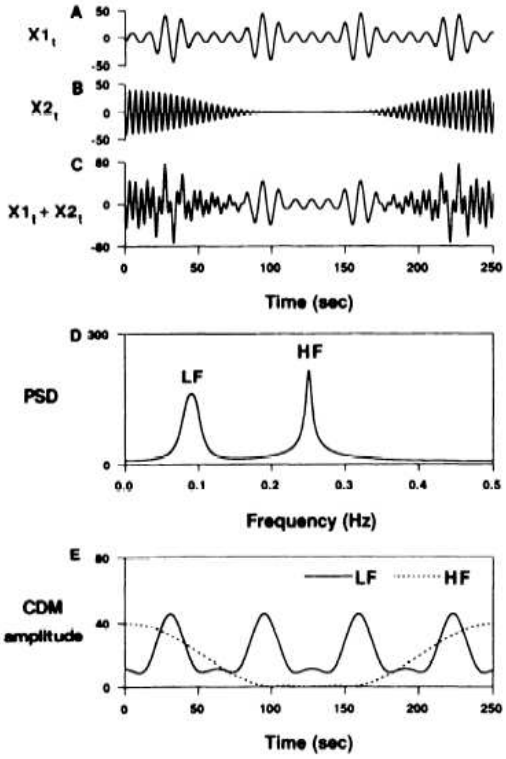

Fig.2.2

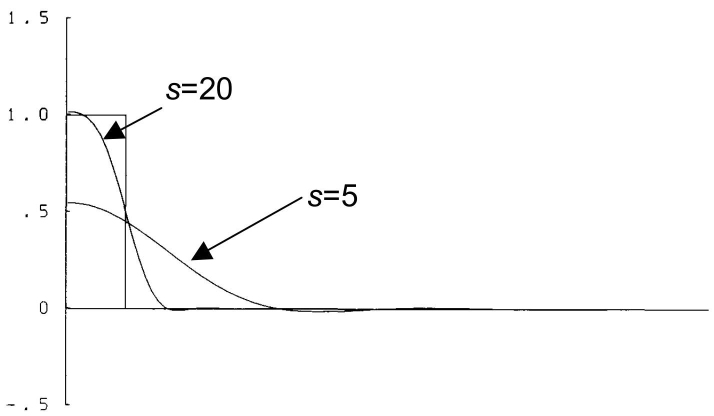

Fig. 2.3

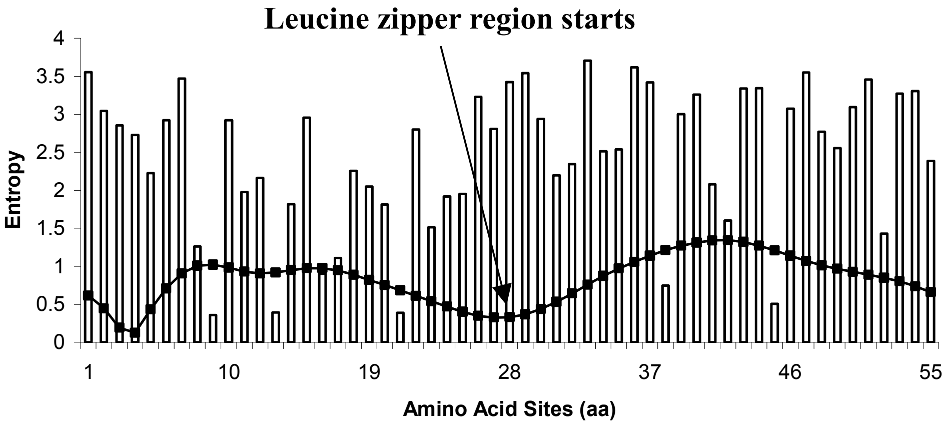

Fig. 2.4

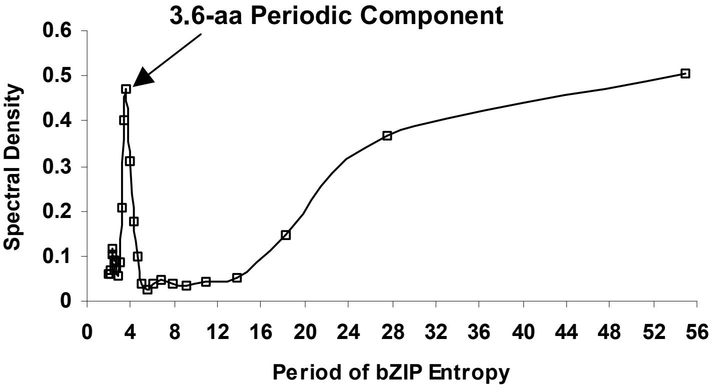

Fig. 2.5

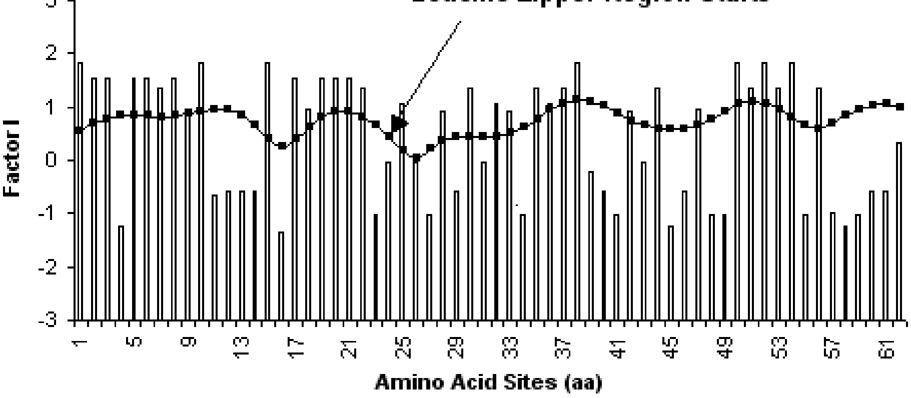

Fig. 2.6

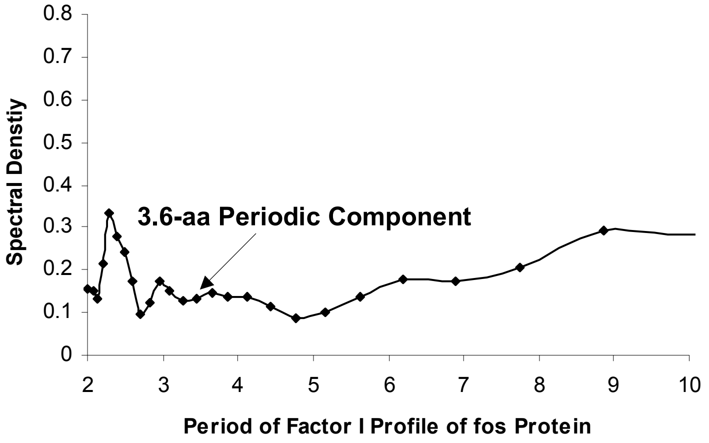

Fig. 2.7

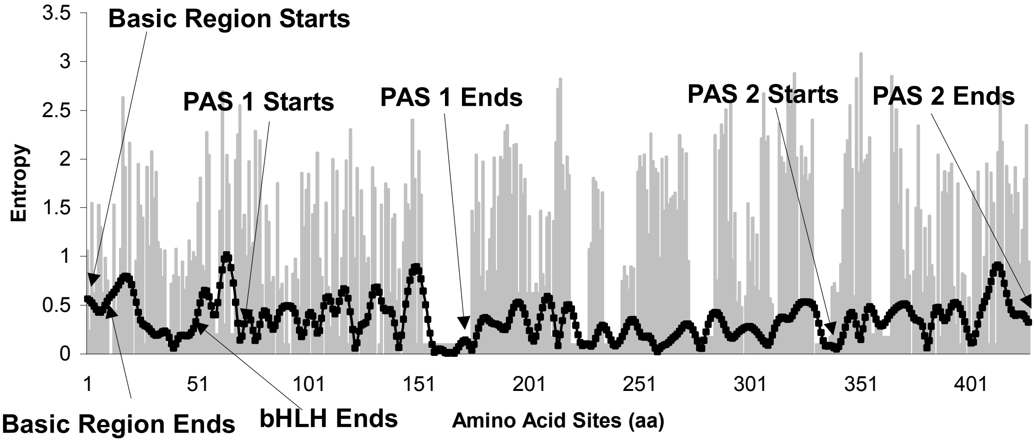

Fig. 2.8

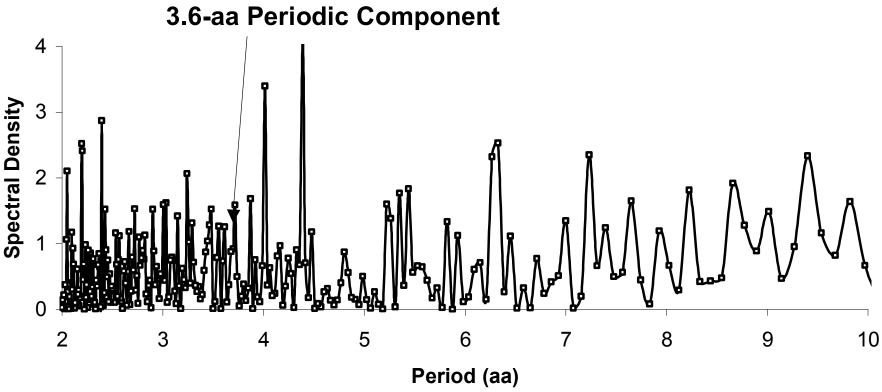

Fig. 2.9

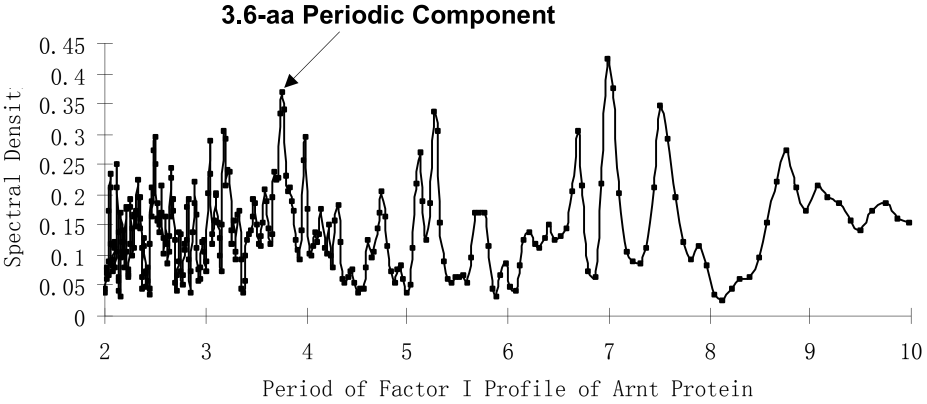
3.6-aa Periodic Component

Fig. 2.10

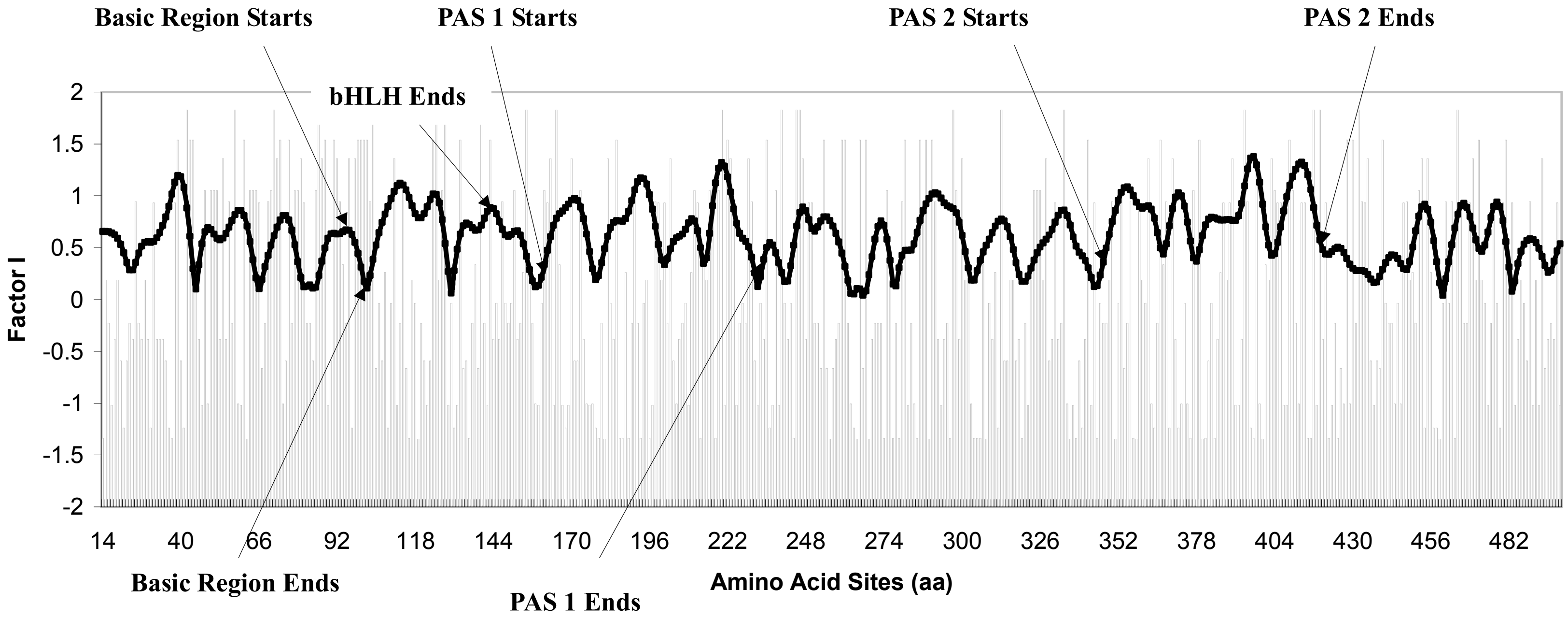
Basic Region Starts
PAS 1 Starts
PAS 2 Starts
PAS 2 Ends
bHLH Ends
2
1.5
1
0.5
0
-0.5
-1
-1.5
-2
Factor I
14
40
66
92
118
144
170
196
222
248
274
300
326
352
378
404
430
456
482
Basic Region Ends
PAS 1 Ends
Amino Acid Sites (aa)

Figure Legends

Fig. 2.1 Comparison between autoregressive power spectrum analysis and complex demodulation (CDM) of simulated data containing two periodic components A and B. A: simulated low-frequency (LF) component. B: simulated high-frequency (HF) component. $X1_t$ and $X2_t$, 0.09 and 0.25 Hz sine functions with a fluctuating amplitude, respectively. C: time series generated by adding 2 sine functions ($X1_t$ +$X2_t$). D: autoregressive power spectrum density (PSD). E: time series of instantaneous amplitude of LF and HF components obtained by CDM. (Figure from Hayano *et al.*, 1993)

Fig. 2.2 Transfer functions of least squares low-pass filters with convergence factors applied, *s*=5 and *s*=20 (Figure from Bloomfield, 1976)

Fig. 2.3 Entropy profile of bZIP protein domains and the amplitude of the 3.6-aa periodic component. The entropy profile is represented by the histogram. Large entropy value represents high variation at that residue while small one represents low variation. Basic region: residue 1-27 Leucine zipper region: residue 28-55. The amplitude of the 3.6-aa periodic component vs. amino acid site is in dotted curve produced by CMD method.

Fig. 2.4 Spectral density plot of the entropy profile of bZIP protein domains in the range from 2 to 10aa (the periodic component of around 3.6 aa period is labeled).

Fig. 2.5 Factor I profile of a bZIP protein domain of transcription factor c-fos protein. The amplitude of the periodic component at 3.6 aa vs. amino acid site is in dotted curve produced by CMD method.

Fig. 2.6 Spectral density plot of the factor I profile of a bZIP protein domain of transcription factor c-fos protein in the range from 2 to 10aa (the periodic component of around 3.6 aa period is labeled).

Fig. 2.7 Entropy profile of bHLH-PAS protein domains and the amplitude of the 3.6-aa periodic component. The entropy profile is represented by the histogram. The amplitude of the 3.6-aa periodic component vs. amino acid site is in dotted curve produced by CMD method.

Fig. 2.8 Spectral density plot of the entropy profile of bHLH-PAS protein domains in the range from 2 to 10aa (the periodic component of around 3.6 aa period is labeled).

Fig. 2.9 Spectral density plot of the Factor I profile of Arnt protein in the range from 2 to 10 aa (the periodic component of around 3.6 aa period is labeled).

Fig. 2.10 Factor I profile of Arnt_human protein and the amplitude of the 3.6-aa periodic component (residue 14 - 499, other residues are trimmed in the process of CDM). The changing amplitude as a function of amino acid sites is produced by CDM and plotted as the curve.

Table

Table 2.1 Summary of the locations of local amplitude minimums and maximums of the 3.6 aa periodic component of the Factor I profile. It is found that the local amplitude minimums and maximums often occur in the boundary area of the α-helices and beta-sheets.

Residue	Local Min	Local Max	Location in the secondary structure
102	Y		End of the basic region
158	Y		Close to the start residue 161 of PAS 1 region
344	Y		Close to the start residue 349 of PAS 2 region
143		Y	End of the HLH region
171		Y	End of a helix
273		Y	Between two β-sheets
291		Y	Close to the end of a helix
313		Y	Close to the end of a β-sheet
334		Y	Start of a β-sheet
355		Y	Start of a β-sheet
397		Y	2nd start residue of of a β-sheet

Supplement

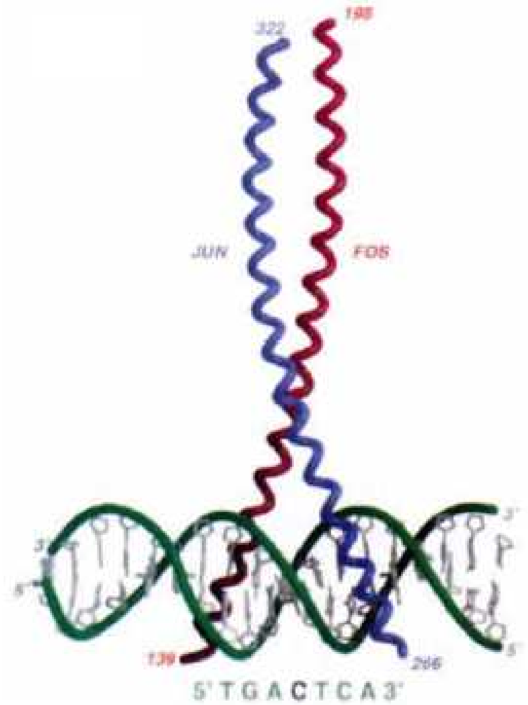

Supplemental Fig. 2.1 Overall Structure of Complex: DNA bended by Fos and Jun bZIP proteins (from Glove, 1995).

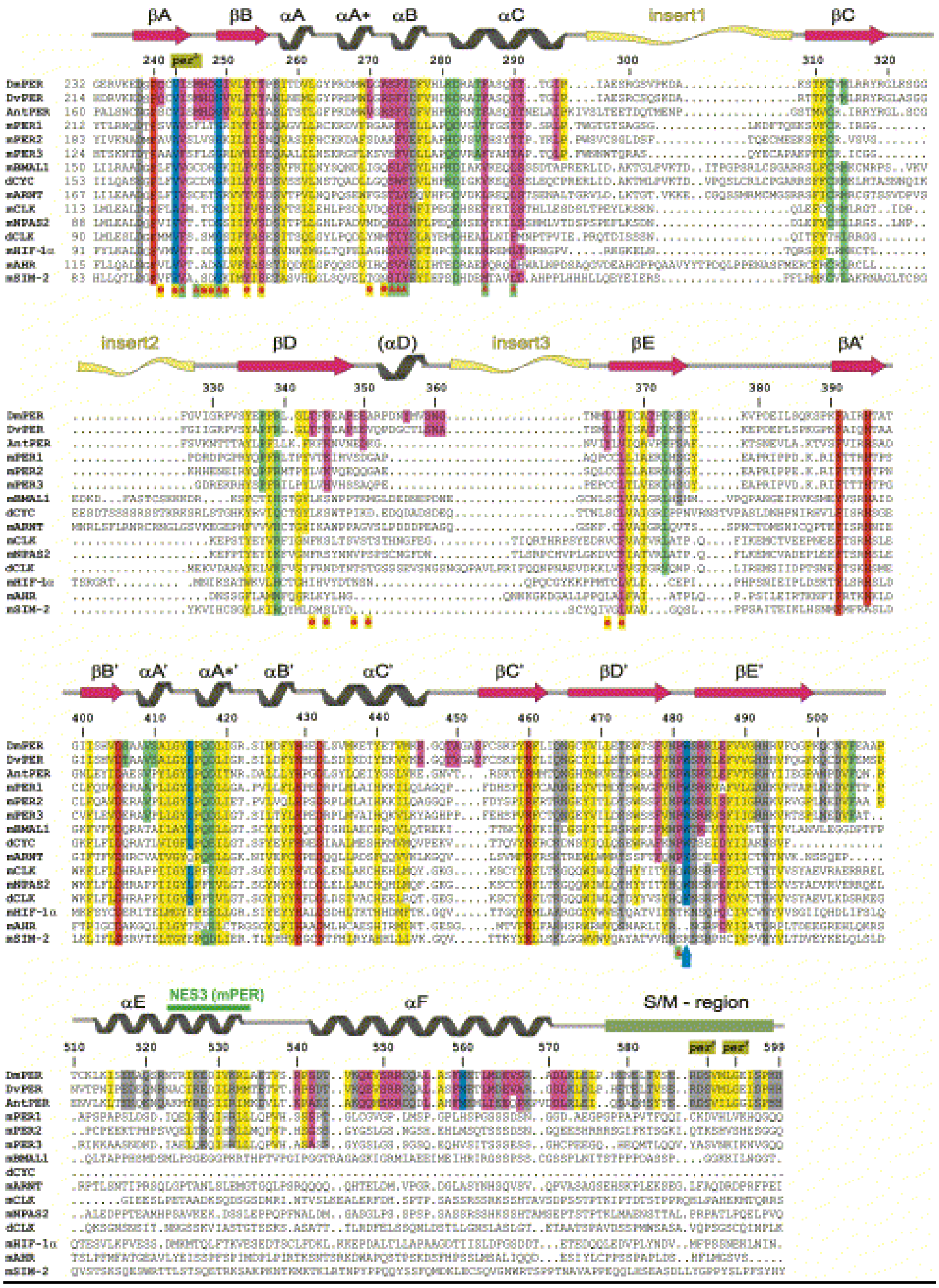

Supplemental Fig.2.2 Structure-Based Sequence Alignment of bHLH-PAS Transcription Factors (from Yildiz, 2005).

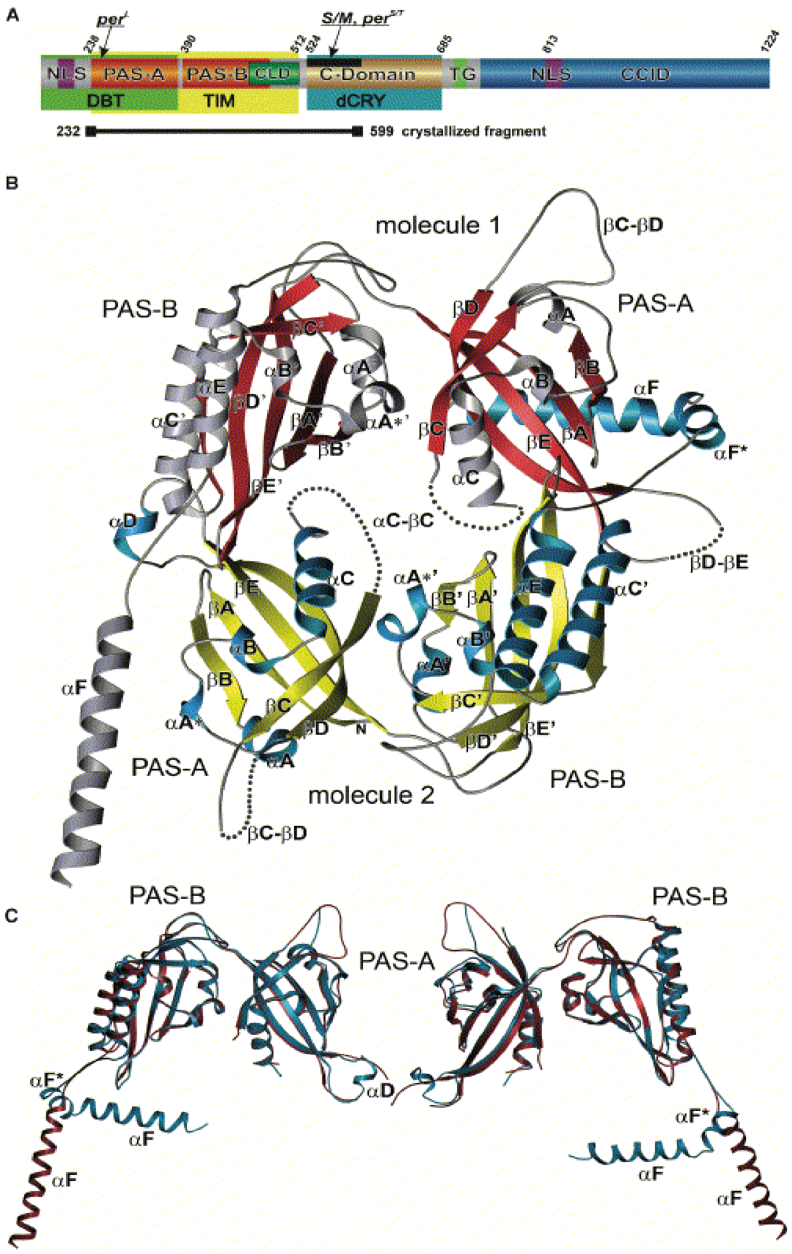

Supplemental Fig.2.3 Domain Architecture and 3D Structure of *Drosophila* Period PAS protein (A) Domain architecture of full-length *Drosophila* PERIOD PAS protein. (B) Ribbon presentation of the Period PAS dimer. Molecule 1 is shown in red and gray, molecule 2 in yellow and blue. (C) Superposition of Period PAS molecules 1 (red) and 2 (blue). Molecule 2 is superimposed onto PAS-2 of molecule 1. (from Yildiz, 2005).

Chapter 3

Evaluation of Amino Acid Indices with Spectral Analysis

by

Zhi Wang[1,*] , William R. Atchley[1,2], Charles E. Smith[1]

[1]Graduate Program In Biomathematics and [2]Department Of Genetics and Center For Computational Biology, North Carolina State University, Raleigh, NC 27695-7614, USA

Keyword: periodicity, spectral analysis, amino acid index

*** To whom correspondence should be addressed**

*** CONTACT: zwang2@ ncsu.edu**

Abstract

It is difficult to select a proper amino acid scale to study protein secondary structure out of the available 494 amino acid indices because some of them are very similar. Till now, there are no comparisons and evaluations of these indices being made. This research proposes a ranking method based on the periodicity parameters of well-known protein sequences. We use a well-know periodicity parameter of a Leucine zipper helix structure to rank the amino acid indices.

Introduction

An amino acid index is defined as a set of 20 numerical values representing any of the different physicochemical and biochemical properties of amino acids. 494 published indices are summarized in a database (http://www.genome.jp/dbget/aaindex.html). As stated in a cluster analysis of amino acid indices for prediction of protein structure and function (Nakai, etc. 1988), all these 492 indices have been clustered into six categories: (i) Alpha and turn propensities (ii) Beta propensity (iii) Composition (iv) Hydrophobicity (v) Physicochemical properties (vi) Other properties. Therefore, many indices are similar with each other or measures of the same physiochemical trait. Such situation could raise some confusion in application. For example, it is difficult to select the hydrophobicity scale because of too many different hydrophobicity indices proposed in the database. Therefore, it is necessary to make evaluation and comparison among those scales based on some well-known structure information of protein sequences.

In this chapter, the α-helix periodicity property of the leucine zipper protein domain is used to evaluate these amino acid scales, who play an important role in the formation of secondary structure. This ranking information should be very useful to promote our secondary structure prediction or develop better bioinformatics tools to understand protein sequences. Those indices that have similar periodicity as that of the secondary structure of protein sequences are assumed as the most useful indices in protein structure prediction.

Materials

The structure of conserved leucine zipper domain of Geminin, a polypeptide of about 25 kDa, occurs in the nuclei of higher eukaryotes and functions as both a negative regulator of genome replication and coordinator of differentiation, has been well studied (Thepaut, 2004). Geminin was discovered as a protein that is degraded when cells exit from mitosis, by the large ubiquitin–ligase complex known as the cyclosome or anaphase-promoting complex, APC.

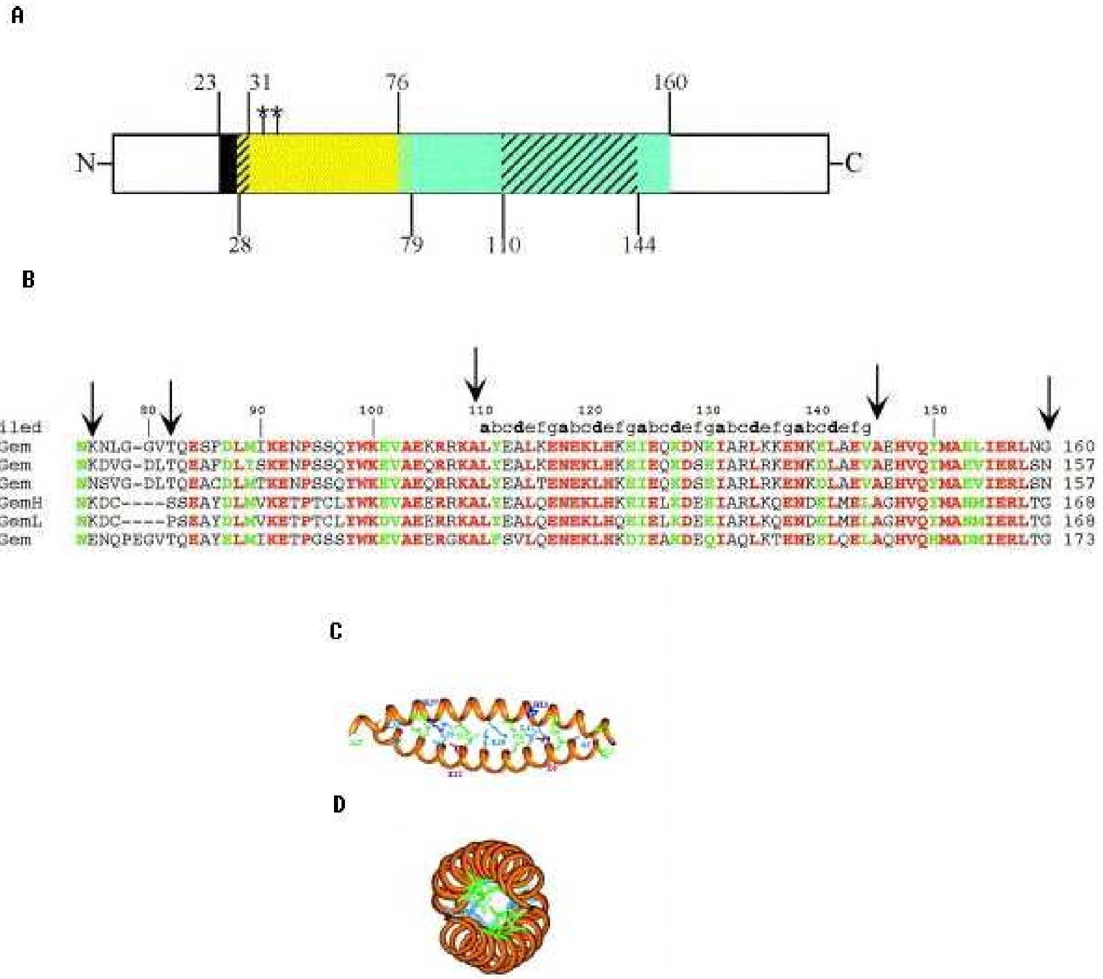
A
23
31
76
160
N
C
28
79
110
144
B
80
90
100
110
120
130
140
150
Coiled abcdefgabcdefgabcdefgabcdefgabcdefg
HsGem NKNLG-GVTQESFDLMIKENPSSQYWKEVAEKRRKALYEALKENEKLHKEIEQKDNEIARLKKENKELAEVAEHVQYMAELIERLNG 160
MmGem NKDVG-DLTQEAFDLISKENPSSQYWKEVAEQRRKALYEALKENEKLHKEIEQKDSEIARLRKENKDLAEVAEHVQYMAEVIERLSN 157
RnGem NNSVG-DLTQEACDLMTKENPSSQYWKEVAEQRRKALYEALTENEKLHKEIEQKDSEIARLRKENKDLAEVAEHVQYMAEVIERLSN 157
XlGemH NKDC----SSEAYDLMVKETPTCLYWKEVAEERRKALYEALQENEKLHKEIELKDEEIARLKQENDELMELAGHVQYMANMIERLTG 168
XlGemL NKDC----PSEAYDLMVKETPTCLYWKDVAEERRKALYEALQENEKLHQEIELKDEEIARLKQENDELMELAGHVQYMANMIERLTG 168
DrGem NENQPEGVTQEAYNLMIKETPGSSYWKEVAEERGKALFSVLQENEKLHKDIEANDEQIAQLKTENEELQELAQHVQHMANMIERLTG 173
C
D

Fig.3.1 Organization, sequence alignment and the structure of human geminin protein domain. (from Thepaut, *et al.,* 2004) (A) Functional domain organization of geminin. The LZ domain is indicated by the hatched area,110–144. (B) Vertebrate geminin sequences alignment of the DNA replication inhibition domain. Letters above the sequences indicate the heptad repeat a,b,c,d,e,f,g positions assigned according to the crystal structure. Strictly conserved residues are in red and similar residues are in green. (C) The overall structure of HsGem-LZ peptide (L2-A37) in $\underline{C^{\alpha}}$ trace representation. (D) Ribbon diagram of the view.

According to the crystal structure analysis (Thepaut, 2004), the structure of the HsGem-LZ peptide is a parallel homodimer coiled coil with a typical α-helical structure. The number of residues per α-helical turn is about 3.64 aa, a value more closely related to a regular α-helix (3.6 aa) than to a classical coiled coil (3.5 aa).

Methods

The HsGem-LZ helices have an periodicity of about 3.64 aa observed from the experimental data. We then transform the HsGem-LZ domain protein sequences into numeric arrays by replacing the alphabetic codes with the 494 indices. Then spectral analysis method (Burg method) has been applied to these numeric sequences to evaluate their periodicities in Matlab. Those indices who have the closest periodicity to 3.64 aa are listed in Table 3.1. Only those periods between the interval (3.458, 3.822) which is within the 5% error range from 3.64 are reported in Table 3.1.

Results

It is found that some indices have a period very close to 3.64 aa and some indices are not. Among those indices, most are related to the formation of secondary structure. A majority of indices falls into the hydrophobicity category, which proved the important role the hydrophobicity plays in the formation of helical structure. This result allows us to do comparison between different hydrophobicity indices and helps us to determine which hydrophobicity scale is the best in terms of secondary structure prediction.

Table 3.1 Ranking of amino acid indices according to the their periodicity estimate of HsGem-LZ protein domain. Only those periods between the interval (3.458, 3.822) which is within the 5% error range from 3.64 are reported here.

Amino Acid Index Name	Series #	Period
Normalized van der Waals volume (Fauchere *et al.*, 1988) P. Physicochemical properties	80	3.6312
Activation Gibbs energy of unfolding, pH9.0 (Yutani *et al.*, 1987) H. Hydrophobicity	396	3.6184
Frequency of the 4th residue in turn (Chou-Fasman, 1978b) A. alpha and turn propensities	52	3.6184
Radius of gyration of side chain (Levitt, 1976) P. Physicochemical properties	157	3.6056
The number of bonds in the longest chain (Charton-Charton, 1983) P. Physicochemical properties	29	3.5930
pK (-COOH) (Jones, 1975) H. Hydrophobicity	133	3.6968
Accessible surface area (Radzicka-Wolfenden, 1988) H. Hydrophobicity	319	3.7101
Optimized transfer energy parameter (Oobatake *et al.*, 1985) H. Hydrophobicity	220	3.5679
Refractivity (McMeekin *et al.*, 1964), Cited by Jones (1975) P. Physicochemical properties	177	3.5679
STERIMOL minimum width of the side chain (Fauchere *et al.*, 1988) P. Physicochemical properties	82	3.5679
Optical rotation (Fasman, 1976) A. alpha and turn propensities	74	3.5556
Distance between C-alpha and centroid of side chain (Levitt, 1976) P. Physicochemical properties	154	3.5433
Residue accessible surface area in tripeptide (Chothia, 1976) H. Hydrophobicity	33	3.5433
STERIMOL length of the side chain (Fauchere *et al.*, 1988) P. Physicochemical properties	81	3.5310
Size (Dawson, 1972) P. Physicochemical properties	63	3.7647
Optimized side chain interaction parameter (Oobatake *et al.*, 1985) H. Hydrophobicity	222	3.5068
Flexibility parameter for two rigid neighbors (Karplus-Schulz,	144	3.7926

1985) C. Composition		
Average relative fractional occurrence in AL(i) (Rackovsky-Scheraga, 1982) C. Composition	302	3.4949
Relative preference value at N4 (Richardson-Richardson, 1988) A. alpha and turn propensities	328	3.4830
Average interactions per side chain atom (Warme-Morgan, 1978) H. Hydrophobicity	382	3.4830
Weights for coil at the window position of -6 (Qian-Sejnowski, 1988) H. Hydrophobicity	284	3.4830
Percentage of exposed residues (Janin *et al*., 1978) H. Hydrophobicity	129	3.4712
Residue accessible surface area in folded protein (Chothia, 1976) H. Hydrophobicity	34	3.4712
Molecular weight (Fasman, 1976) P. Physicochemical properties	72	3.4712
Proportion of residues 100% buried (Chothia, 1976) H. Hydrophobicity	36	3.4595
Transfer free energy (Janin, 1979) H. Hydrophobicity	131	3.4595
Average accessible surface area (Janin *et al*., 1978) H. Hydrophobicity	127	3.4595
Weights for beta-sheet at the window position of -4 (Qian-Sejnowski, 1988) H. Hydrophobicity	273	3.4595
Side chain orientational preference (Rackovsky-Scheraga, 1977) H. Hydrophobicity	299	3.4595

ACKNOWLEDGEMENTS

Thanks to Charles Smith and Jieping Zhao for their helpful suggestions. This research was supported by a grant from the National Institutes of Health (GM45344) to WRA.

Summary

This dissertation describes several powerful computational techniques to conduct spectral analysis on protein sequences. Spectral analysis has not been widely used in protein sequences and it is the first time to apply it to analyze the periodicity of variability pattern of protein domains.

In Chapter 1, spectral analysis is conducted to study the periodicity of the variability pattern of bHLH protein domains represented by the entropy profile. It is found that there is a significant periodic component of about 3.6 aa in the entropy profile, which has implication of the underlying helix structure. In order to understand the physiochemical causes of the variability, we decompose the variability into five factor scores representing i) polarity / hydrophobicity / accessibility, ii) propensity for various secondary structures, iii) molecular volume, iv) codon composition and v) electrostatic charge. The periodicities of these factor means/variances profiles also have implications of the helix structure.

In Chapter 2, complex demodulation method (CDM) is a complementary method of the spectral analysis method used in Chapter 2 because it can describe the changing amplitude of a certain frequency of the data. And therefore, it can provide very meaningful information that FFT method cannot provide. Although CDM has been widely applied into other scientific fields, it is the first report that CDM has been introduced into computational biology. With the analysis of bZIP protein domains

and more complex bHLH-PAS protein domains, CDM proves to be a very useful technique of description of the amplitude of a certain frequency. The analyses on the amplitude of the periodic component of about 3.6 aa reveal that the local maximums/minimums have implications of the boundary of the secondary structure α-helix and β-sheet. For bZIP protein domain, the CDM method can separate the basic region and ZIP region very well. And even there are no significant 3.6-aa periodic components in the bZIP Factor I profile, CDM still shows some robustness to indicate the boundary of the basic region and the ZIP region.

In Chapter 3, spectral analysis is conducted to evaluate and compare the amino acid indices to see if their periodicity property conforms to the observed 3.64-aa periodicity of a Leucine Zipper domain. It seems that the periodicity parameter can be a criteria of selecting a proper amino acid index for the goal of studying protein structure, function and evolution. In this way, the redundancy of the amino acid indices can be largely reduced.

REFERENCE

Atchley, W. R. and Fitch, W. M. (1997) A natural classification of the basic helix-loop-helix class of transcription Factors. *Proc. Natl. Acad. Sci. USA*, 94, 5172-5176.

Atchley, W. R., *et al.* (1999) Positional Dependence, cliques and predictive motifs in the bHLH protein domain. *J. Mol. Evol.* 48:501-519.

Atchley, W.R., *et al.* (2000) Correlations among amino acid residues in bHLH protein domains: An information theoretic analysis. *Mol. Biol. Evol.* 17, 164-178.

Atchley, W.R., *et al.* (2005) Solving the protein sequence “metric” problem. *Proc. Natl. Acad. Sci. USA* 102, 6395-6400.

Atchley WR, Fernandes AD. (2005) Sequence signatures and the probabilistic identification of proteins in the Myc-Max-Mad network. *Proc Natl Acad Sci* 102, 6401-6406.

Babkoff H, Caspy T, Mikulincer M, Sing HC. (1991) Monotonic and rhythmic influences: a challenge for sleep deprivation research. *Psychol Bull.*109, 411-428

Bloomfield, P. (1976) *Fourier analysis of time series: An introduction*. Wiley, New York. pp.1-150

Brockwell, P.J., and Davis, R.A. (1991). *Time Series: Theory and Methods (2nd ed).* Springer Verlag. section 10.2

Brownlie, P., Ceska, T., Lamers, M., Romier, C., Stier, G., Teo, H. & Suck, D. (1997) The crystal structure of an intact human Max-DNA complex: new insights into mechanisms of transcriptional control. *Structure*. 5, 509-520.

Buck, M.J. (2003) *Protein evolution from sequence to structure.* (Ph.D. thesis) pp.49-50, North Carolina State University, USA

Buck M.J., Atchley W.R., (2005) Networks of coevolving sites in structural and functional domains of serpin proteins. *Mol Biol Evol.* 22,1627-1634

Chou, P.Y. and Fasman, G.D. (1978) Prediction of the secondary structure of proteins from their amino acid sequence *Adv. Enzymol.* 47, 45-148

Charton, M. and Charton, B. (1983) The dependence of the Chou-Fasman parameters on amino acid side chain structure *J. Theor. Biol.* 111, 447-450

Chothia, C. (1976) The nature of the accessible and buried surfaces in proteins *J. Mol. Biol.* 105, 1-14

Wilson C. L., Boardman P. E., Doig A. J., Hubbard S. J., (2004) Improved prediction for N-termini of α-helices using empirical information *Proteins: Structure, Function, and Bioinformatics* 57 ,322 – 330

Dawson, D.M. (1972) The Biochemical Genetics of Man Academic Press, New York, pp.1-38

Eisenburg, D., *et al.* (1984) The hydrophobic moment detects periodicity in protein Hydrophobicity. *Proc. Natl. Acad. Sci. USA*, 81, 140-144.

Fasman, G.D., (1976) "Handbook of Biochemistry and Molecular Biology", 3rd ed., Proteins Volume 1, CRC Press, Cleveland

Fasman, G.D., (1989) Prediction of protein structure and the principles of protein conformation *Plenum Press, New York pp. 625-646*

Fauchere, J.L., Charton, M., Kier, L.B., Verloop, A. and Pliska, V. (1988) Amino acid side chain parameters for correlation studies in biology and pharmacology *Int. J. Peptide Protein Res.* 32, 269-278

Ferre-D'Amare A.R., Prendergast G.C., Ziff E.B., Burley S.K. (1993) Recognition by Max of its cognate DNA through a dimeric b/HLH/Z domain. *Nature* 363,38–45

Glover J.N., Harrison S.C., (1995) Crystal structure of the heterodimeric bZIP transcription factor c-Fos-c-Jun bound to DNA. *Nature* 373:257-261

Grantham,R., (1974) Amino acid difference formula to help explain protein evolution. *Science* 185, 862-864.

Hamming, R.W. (1983) *Digital filters* (2nd ed.). Prentice Hall, Englewood Cliffs, New Jersey.

Hayano J, Taylor JA, Yamada A, Mukai S, Hori R, Asakawa T, Yokoyama K, Watanabe Y, Takata K, Fujinami T. (1993) Continuous assessment of hemodynamic control by complex demodulation of cardiovascular variability. *Am J Physiol*. 264 1229-1238.

Hefti MH, Francoijs KJ, de Vries SC, Dixon R, Vervoort J, (2004) The PAS fold: a redefination of the PAS domain based upon structural prediction. *Eur J Biochem* 271:1198-1208.

Herzel H., Weiss O., Trifonov E.N. (1999) 10-11 bp periodicities in complete genomes reflect protein structure and DNA folding. *Bioinformatics*. 15,187-193.

Hoffman,E.C., Reyes,H., Chu,F.F., Sander,F., Conley,L.H., Brooks,B.A. and Hankinson,O. (1991) Cloning of a factor required for activity of the Ah (dioxin) receptor *Science* 252 (5008), 954-958

Janin, J., Wodak, S., Levitt, M., and Maigret, B. (1978) Conformation of amino acid side-chains in proteins *J. Mol. Biol.* 125, 357-386

Janin, J. (1979) Transfer free energ Surface and inside volumes in globular proteins *Nature* 277, 491-492

Johnson and Wichern (2002) Applied Multivariate Analysis, 5/e, Prentice Hall

Jones, D.D. (1975) Amino acid properties and side-chain orientation in proteins: A cross correlation approach *J. Theor. Biol.* 50, 167-183

Karplus, P.A. and Schulz, G.E. (1985) Prediction of chain flexibility in proteins. Naturwissenchaften 72, 212–213.

Kay, S. M. (1988) *Modern Spectral Estimation: Theory and Application*, Prentice Hall, Englewood Cliffs, New Jersey. pp. 265-270

Kendall, M. and Ord, J.K. (1990) *Time series* Edward Arnold, Sevenoaks, Kent, Great Britain pp.51-52, 170

Kyte, J. (1995) *Structure in Protein Chemistry* Garland Publishing, Inc., New York and London pp.201

Ledent V, Vervoort M (2001) The basic helix-loop-helix protein family: comparative genomics and phylogenetic analysis. *Genome Res* 11,754–770

Leonov, H. and Arkin, I.T. (2005) A periodicity analysis of transmembrane helices *Bioinformatics* 21, 2604-2610

Levitt, M. (1976) A simplified representation of protein conformations for rapid simulation of protein folding *J. Mol. Biol.* 104, 59-107

Lipsitz LA, Hayano J, Sakata S, Okada A, Morin RJ. (1998) Complex demodulation of cardiorespiratory dynamics preceding vasovagal syncope. *Circulation.* 98(10):977-983.

Marple, S. L. (1987) *Digital Spectral Analysis with Applications*, Prentice Hall, Englewood Cliffs, New Jersey. pp.21, 164, 172-284, 379

McMeekin, T.L., Groves, M.L., and Hipp, N.J. (1964) In "Amino Acids and Serum Proteins" (Stekol, J.A., ed.), American Chemical Society, Washington, D.C., p. 54

Morgenstern B, Atchley WR (1999) Evolution of bHLH transcription factors: modular evolution by domain shuffling? *Mol Biol Evol* 16,1654–1663

Murre, C., *et al.* (1989) A new DNA binding and dimerization motif in immunoglobulin enhancer binding, daughterless, MyoD, and myc proteins. *Cell* 56, 777–783.

Murre, C, *et al.* (1994) Structure and function of helix-loop-helix proteins *Biochim. Biophys. Acta* 1218, 129–135.

Naidu, P. S. (1996) *Modern Spectrum Analysis of Time Series*, pp. 161-162, 241, CRC press, Boca Raton, Florida.

Nakai, K., Kidera, A., and Kanehisa, M.; (1988) Cluster analysis of amino acid indices for prediction of protein structure and function. *Protein Eng.* 2, 93-100.

Oobatake, M., Kubota, Y. and Ooi, T. (1985) Optimization of amino acid parameters for correspondence of sequence to tertiary structures of proteins *Bull. Inst. Chem. Res.,* Kyoto Univ. 63, 82-94

Pasquier, C.M., *et al.* (1998) A web server to locate periodicities in a sequence. *Bioinformatics*. 14, 749-750.

Patthy, L. (1999) *Protein Evolution*. Blackwell Science ltd., Oxford pp.42-43

Percival, D. B.& Walden, A. T. (1993) *Spectral Analysis for Physical Applications*, pp. 414, 445-449, Cambridge University Press, New York.

Podust LM, Krezel AM, Kim Y. (2001) Crystal structure of the CCAAT box/enhancer-binding protein beta activating transcription factor-4 basic leucine zipper heterodimer in the absence of DNA. *J Biol Chem.* 276(1):505-13.

Ponting C.P., Aravind L., (1997).PAS: a multifunctional domain family comes to light. *Curr. Biol.* 7:R674-R677

Qian, N. and Sejnowski, T.J. (1988) Predicting the secondary structure of globular proteins using neural network models *J. Mol. Biol.* 202, 865-884

Quinn, L.M., A. Herr, T.J. McGarry and H. Richardson, (2001) The Drosophila Geminin homolog: roles for Geminin in limiting DNA replication, in anaphase and in neurogenesis, *Genes Dev.* 15 pp. 2741–2754

Rackovsky, S. and Scheraga, H.A. (1977) Hydrophobicity, hydrophilicity, and the radial and orientational distributions of residues in native proteins *Proc. Natl. Acad. Sci.* USA 74, 5248-5251

Rackovsky, S. and Scheraga, H.A. (1982) Differential geometry and polymer conformation. 4. Conformational and nucleation properties of individual amino acids Macromolecules 15, 1340-1346

Radzicka, A. and Wolfenden, R. T (1988) Comparing the polarities of the amino acids: Side-chain distribution coefficients between the vapor phase, cyclohexane, 1-octanol, and neutral aqueous solution *Biochemistry* 27, 1664-1670

Richardson, J.S. and Richardson, D.C. (1988) Amino acid preferences for specific locations at the ends of alpha helices *Science* 240, 1648-1652

Rutherford S, D'Hondt S., (2000) Early onset and tropical forcing of 100,000-year Pleistocene glacial cycles. *Nature.* 408, 72-75.

SAS, (1992) *SAS/ETS Software Application Guide 1*. SAS Institute Inc., Cary, NC, USA pp.220 http://v9doc.sas.com/sasdoc/

Sauve S, Tremblay L, Lavigne P. (2004) The NMR solution structure of a mutant of the Max b/HLH/LZ free of DNA: insights into the specific and reversible DNA binding mechanism of dimeric transcription factors. *J Mol Biol.* 342(3): 813-32.

Schieg P., Herzel H., (2004) Periodicities of 10-11bp as indicators of the supercoiled state of genomic DNA. *J Mol Biol.* 343 (4):891-901

Shannon, C.& Weaver, W. (1949) *The Mathematical Theory of Communication*. University of Illinois Press, Urbana.

Sharma, D., Issac, B., Raghava, G.P. & Ramaswamy, R. (2004) Spectral Repeat Finder (SRF): identification of repetitive sequences using Fourier transformation. *Bioinformatics*. 20, 1405-1412

Shimizu T, Toumoto A, Ihara K, Shimizu M, Kyogoku Y, Ogawa N, Oshima Y, Hakoshima T. (1997) Crystal structure of PHO4 bHLH domain-DNA complex: flanking base recognition. *EMBO J*. 16(15): 4689-97.

Sneath P.H.A., (1966) Relations between chemical structure and biological activity. *J Theor Biol* 12:157–195

Sun, X. and Baltimore, D. (1991) An inhibitory domain of E12 transcription factor prevents DNA binding in E12 homodimers but not in E12 heterodimers. *Cell* 64, 459–467.

Thepaut, M., Maiorano, D., Guichou, J.F., Auge, M.T., Dumas, C., Mechali, M., Padilla, A. (2004) Crystal structure of the coiled-coil dimerization motif of geminin: structural and functional insights on DNA replication regulation. *J Mol Biol.* 342, 275-87

Warme, P.K. and Morgan, R.S. (1978) A survey of amino acid side-chain interactions in 21 proteins *J. Mol. Biol.* 118, 289-304

Warner, R. M. (1998) *Spectral Analysis of Time-Series Data*, The Guilford Press, New York, London. pp. 1-111.

Wilson, C.L., Boardman, P.E., Doig, A.J., Hubbard, S.J. (2004) Improved prediction for N-termini of alpha-helices using empirical information. *Proteins.* 57, 322-330

Wollenberg, K.R. and Atchley, W.R. (2000) Separation of phylogenetic and functional associations in biological sequences by using the parametric bootstrap. *Proc. Natl. Acad. Sci.* 97,3288-3291.

Yutani, K., Ogasahara, K., Tsujita, T., and Sugino, Y. (1987) Dependence of conformational stability on hydrophobicity of the amino acid residue in a series of variant proteins substituted at a unique position of tryptophan synthase alpha subunit *Proc. Natl. Acad. Sci.* USA 84, 4441-4444

Zhulin I.B., Taylor B.L., Dixon R., (1997) PAS domain S-boxes in Archaea, Bacteria and sensors for oxygen and redox. *Trends Biochem. Sci.* 22:331-333

Appendix A: Spectral Analysis Based on the Burg Method

The procedure of Burg method is briefly described here. For more details, please refer to the books by Kay, 1988 and Marple, 1987. Spectral analysis is applied to determine the spectral content of a random process based on a finite set of observations from that process. The power spectral density (PSD denoted by *P_{xx}*(*f*) , of a complex wide sense stationary (WSS) random process *x*[*n*] is defined as

$$p_{xx}(f) = \sum_{k=-\infty}^{\infty} r_{xx}[k]\exp(-j2\pi fk) \qquad -\frac{1}{2} \le f \le \frac{1}{2}$$

Where $r_{xx}[k]$ is the autocorrelation function (ACF) of *x*[*n*] defined as

$$r_{xx}[k] = E\ (\ x^*[n]x[n+k]\ )$$

E is expectation operator. The PSD function describes the distribution of power with frequency of the random process.

When the autoregressive (AR) modeling assumption is valid, spectral estimators are obtained which are less biased and have a lower variability than conventional Fourier based spectral estimators. To estimate the PSD using an AR model we need to estimate the parameters of the model. The theoretical PSD is given as below

$$p_{AR}(f) = \frac{\sigma^2}{\left|1 + a[1]\exp(-j2\pi f) + ... + a[p]\exp(-j2\pi f)\right|^2}$$

The estimate of the PSD is obtained by replacing the theoretical AR parameters by their estimates to yield

$$\hat{p}_{AR}(f) = \frac{\hat{\sigma}^2}{\left|1 + \hat{a}[1]\exp(-j2\pi f) + ... + \hat{a}[p]\exp(-j2\pi f)\right|^2}$$

In order to estimate AR parameters, the basic idea is to minimize the average of the forward and backward prediction error.

Forward predictor $\hat{x}^f[n] = \sum_{k=1}^{p} a^f[k]x[n-k]$

Backward predictor $\hat{x}^b[n] = \sum_{k=1}^{p} a^b[k]x[n-k]$

Minimization of the average errors yields an optimal estimate of K_k

$$\hat{k}_k = \frac{-2\sum_{n=k}^{N-1} \hat{e}^f_{k-1}[n]\hat{e}^b_{k-1}[n-1]^*}{\sum_{n=k}^{N-1}\left(\left|\hat{e}^f_{k-1}[n]\right|^2 + \left|\hat{e}^b_{k-1}[n-1]\right|^2\right)}$$

where *e* is the prediction error

This $\hat{k}_k$ is used in each stage of the Levinson-recursive algorithm to produce $\hat{a}[1]$, $\hat{a}[2]$,…, and $\hat{a}[p]$

Appendix B: Critical Values for the Fisher Test of Significance

The critical values in Tables B.1 and the description of Fisher Test presented below are from Warner (1998).

To compute the test statistic *g*, compute the periodogram for the time series. Find the sum of all the periodogram ordinates, and then divide the periodogram intensity for each frequency by this sum to yield an estimate of the proportion of variance in the time series that is accounted for by each frequency component represented in the periodogram. The test statistic *g* is simply the proportion of the total variance in the time series that is accounted for by a particular frequency in the periodogram analysis.

Select the largest values of this proportion, that is, the proportions of variance that are explained by the first largest, second largest, third largest, fourth largest, and fifth largest periodogram ordinates. The tables provided here give critical values to test the significance of the peaks that are ranked first through fifth largest in the proportion of variance accounted for.

To choose the appropriate critical values, you need to know *N* (number of observations in the time series), and the alpha level for your significance tests. Critical values of *g* are given for α = .05 in Table B.1. Within the table, the columns headed r1, r2, r3, r4, and r5 give the critical values used to test the significance of the peaks that are ranked first, second, …,fifth in the periodogram.

Start with the largest obtained proportion of variance and compare this to the critical value in the r1 column (critical value of *g* for the largest periodogram ordinate). If the obtained proportion of variance exceeds the critical value given in the table then this first peak is statistically significant. Smaller peaks may be tested only if the larger peaks were significant.

TABLE B.1. Critical Values of the Proportion of Variance for the Fisher Test, α = .05

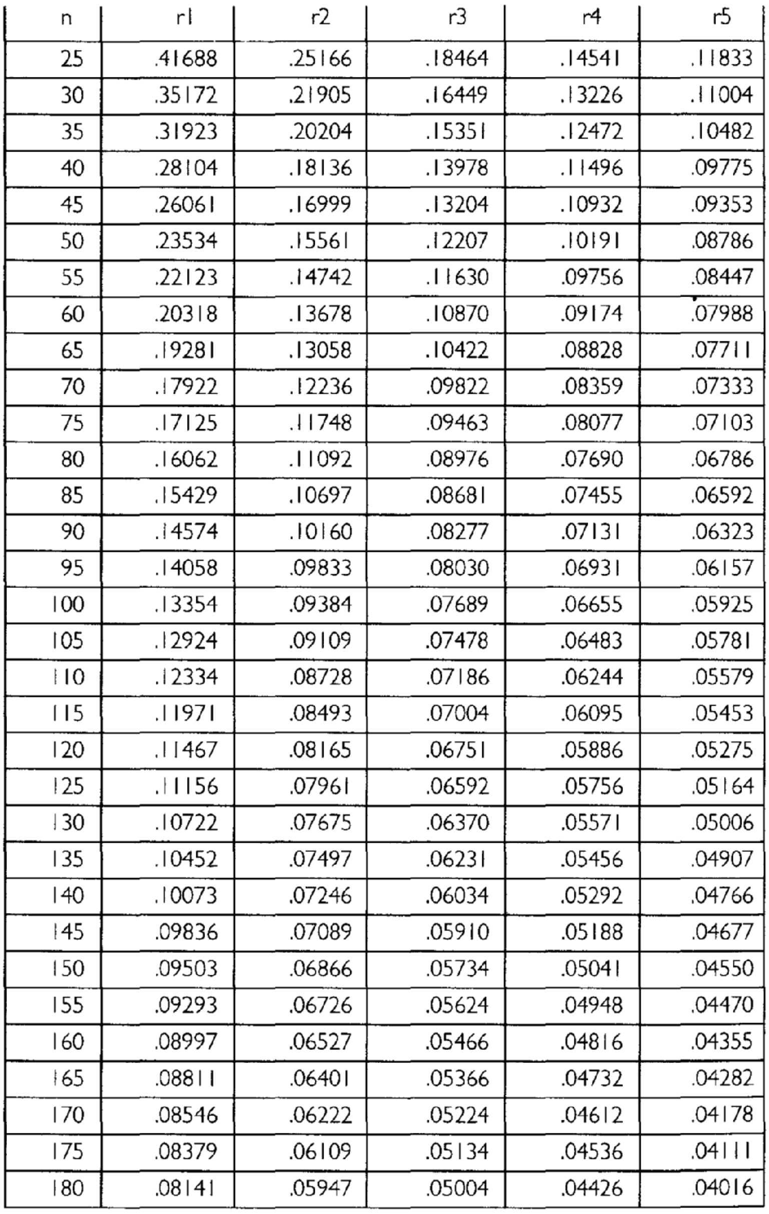

n	r1	r2	r3	r4	r5
25	.41688	.25166	.18464	.14541	.11833
30	.35172	.21905	.16449	.13226	.11004
35	.31923	.20204	.15351	.12472	.10482
40	.28104	.18136	.13978	.11496	.09775
45	.26061	.16999	.13204	.10932	.09353
50	.23534	.15561	.12207	.10191	.08786
55	.22123	.14742	.11630	.09756	.08447
60	.20318	.13678	.10870	.09174	.07988
65	.19281	.13058	.10422	.08828	.07711
70	.17922	.12236	.09822	.08359	.07333
75	.17125	.11748	.09463	.08077	.07103
80	.16062	.11092	.08976	.07690	.06786
85	.15429	.10697	.08681	.07455	.06592
90	.14574	.10160	.08277	.07131	.06323
95	.14058	.09833	.08030	.06931	.06157
100	.13354	.09384	.07689	.06655	.05925
105	.12924	.09109	.07478	.06483	.05781
110	.12334	.08728	.07186	.06244	.05579
115	.11971	.08493	.07004	.06095	.05453
120	.11467	.08165	.06751	.05886	.05275
125	.11156	.07961	.06592	.05756	.05164
130	.10722	.07675	.06370	.05571	.05006
135	.10452	.07497	.06231	.05456	.04907
140	.10073	.07246	.06034	.05292	.04766
145	.09836	.07089	.05910	.05188	.04677
150	.09503	.06866	.05734	.05041	.04550
155	.09293	.06726	.05624	.04948	.04470
160	.08997	.06527	.05466	.04816	.04355
165	.08811	.06401	.05366	.04732	.04282
170	.08546	.06222	.05224	.04612	.04178
175	.08379	.06109	.05134	.04536	.04111
180	.08141	.05947	.05004	.04426	.04016